1.0

4.5
5.0

2.8

2.5

3.2

2.2

3.6

1.1

4.0

2.0

1.8

1.25

1.4

1.6

MICROCOPY RESOLUTION TEST CHART

NATIONAL BUREAU OF STANDARDS 1963 A

LEVEL

AD A099816

# A Moments Approach for Analyzing Geophysical Reflection Data

Norman H. Gholson
Martin G. Faget

Ocean Technology Division
Ocean Science and Technology Laboratory

May 1981

Distribution Unlimited

45

392 773

81 6 08 066

# Foreword

A new approach for analyzing
geophysical acoustic reflection data
has been developed. The approach,
labeled a "moments" approach, provides
a simple method of estimating source to
receiver travel times for a laterally
homogeneous medium with an arbitrary
sound speed versus depth relationship.
Estimating a sound speed versus depth
relationship from measured travel time
data is also addressed. The effort
described in this document was per-
formed in support of NORDA's Deep-
Towed Geophysical Array System
Program.

*D. D. Phelps*

G. T. Phelps, Captain, USN
Commanding Officer
NORDA

This publication presents a new
approach developed for analyzing
geophysical acoustic reflection data.
The forward problem of estimating
source to receiver travel time, and the
inverse problem of estimating a sound
speed versus depth relationship are
addressed using a moments approach.
The moments approach provides a simple
tool for estimating source to receiver
reflection path travel time for a
laterally homogeneous medium with an
*arbitrary* sound speed versus depth
relationship. The moments approach
also provides a useful tool for
inverting reflection data to obtain an
estimate of the sound speed versus
depth relationship. A nearly closed
form technique for estimating a *linear*
sound speed versus depth relationship
is presented. Derivation of the
moments approach and numerical examples
are included.

DTIC
SELECTED
JUN8 1981

D

# Contents

# Illustrations and Tables

## Illustrations

## Tables

# A Moments Approach for Analyzing Geophysical Reflection Data

## I. Introduction

Geophysical reflection data can be analyzed to estimate compressional sound speed as a function of depth. Utility of such data may be subtle or quite straightforward; exact details are beyond the scope of this document. Analysis presented in this report is confined to a laterally homogeneous medium with non-sloping reflecting boundaries.

Acoustic reflection data are typically acquired using a measurement system geometry similar to that shown in Figure 1. The source provides a series of acoustic energy pulses which propagate through the medium of interest to an array of acoustic receivers. The distinctive feature of acoustic reflection data is that the received energy arrives via a reflection phenomenon. The reflection phenomenon is caused by an abrupt change in acoustic impedance at layer boundaries. Example reflection paths are illustrated by paths $SR_{1,1}$, $SR_{3,1}$, $SR_{1,2}$ of Figure 1, where $SR_{i,j}$ denotes the reflection path from source to receiver i from reflecting boundary j.

Analyzing acoustic reflection data to determine sound speed as a function of depth (z coordinate in Figure 1) requires two important tools. The first tool is a technique for estimating reflection path travel time from source to receiver for candidate sound speed versus depth relationships. The second tool is the inverse of the first, in that the second tool is a technique for processing measured travel time data to estimate the sound speed versus depth relationship. This report describes a moments approach for handling the forward problem (travel time from known sound speed profile) and inverse problem (sound speed profile from known travel time data).

The forward problem is handled in a general sense by considering an *arbitrary* sound speed versus depth relationship. Treatment of the inverse problem is not so general, but is distinguished in that a *nearly closed* form technique of estimating a linear sound speed versus depth relationship is presented. The following sections of this report define the "moments" of a sound speed versus depth relationship and illustrate utility of the approach for processing geophysical acoustic reflection data.

## II. Moments of a Sound Speed Profile

The compressional sound speed profile will be denoted by $V_Z(z)$ where $z$ is the depth coordinate ($z = 0$ at the source). As discussed earlier, the analysis presented in this report considers the case where sound speed is a function of depth only (laterally homogeneous medium).

Moments of a sound speed versus depth relationship, $V_Z(z)$, for a particular measurement configuration are defined with the aid of Figure 2. The $i^{th}$ moment*, $M_i$, is defined as follows.

---

*Moments of a sound speed vs. depth relationship should not be confused with moments of a probability density function (statistics) or moments of a mass distribution (mechanics). The particular label "moments" was chosen because of slight similarities to statistical and mechanical definitions.
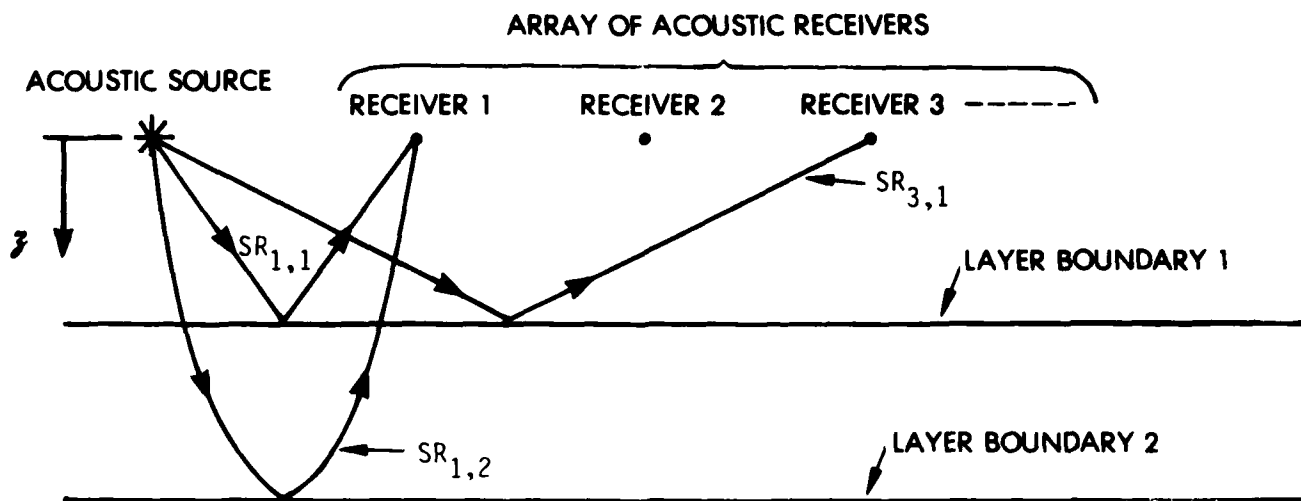
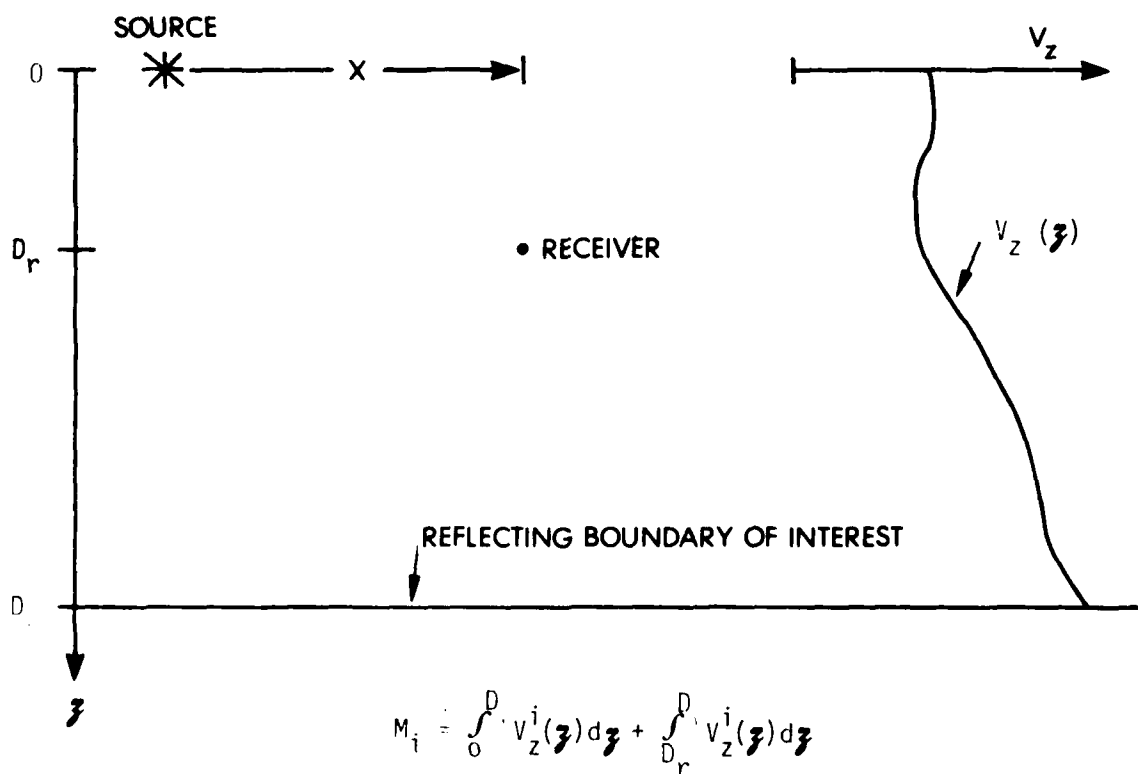Figure 1. Measurement System Geometry



$$M_i = \int_0^D V_z^i(\mathbf{z}) d\mathbf{z} + \int_{D_r}^D V_z^i(\mathbf{z}) d\mathbf{z}$$

Figure 2. Defining Moments

$$M_i \triangleq \int_0^{D_\ell} V_Z^i(\mathbf{z})d\mathbf{z} + \int_{D_r}^{D_\ell} V_Z^i(\mathbf{z})d\mathbf{z} \qquad (1a)$$

where $\mathbf{z} \triangleq$ depth below source,

$V_Z(\mathbf{z}) \triangleq$ sound speed as a function of $\mathbf{z}$,

$D_\ell \triangleq \mathbf{z}$ coordinate of reflecting boundary and

$D_r \triangleq \mathbf{z}$ coordinate of acoustic receiver.

For the case where source and receiver are at the same depth ($D_r = 0$), the moments definition reduces to

$$M_i \triangleq 2 \int_0^{D_\ell} V_Z^i(\mathbf{z})d\mathbf{z} \qquad (1b)$$

Without regard to their utility, it is beneficial to notice the simplicity of computing moments for a sound speed profile $V_Z(\mathbf{z})$. As an example, consider the source and receiver geometry of Figure 3 with a $V_Z(\mathbf{z})$ consisting of a constant *gradient* (linear sound speed versus depth relationship) layer and a constant sound speed layer. From defining equation (1b), $M_i$ for the case displayed in Figure 3 becomes

$$M_i = 2 \int_0^{D_1} (V_0 + g\mathbf{z})^i \, d\mathbf{z} + 2 \int_{D_1}^{D_2} V_c^i \, d\mathbf{z}. \qquad (2)$$

Evaluating equation (2) results in the following.

$$M_i = \frac{2}{g} \ln\left(\frac{V_0 + gD_1}{V_0}\right) + \frac{2(D_2 - D_1)}{V_c} \quad \text{for } i = -1 \text{ and}$$

$$M_i = 2\left[\frac{(V_0 + gD_1)^{i+1} - V_0^{i+1}}{(i+1)g} + V_c^i(D_2 - D_1)\right] \text{ for } i \neq -1 ,$$

where $\ln(.)$ denotes natural log.

Additional examples are given in Appendix A. The important feature to be noted is that moments can be calculated quite easily for virtually any $V_Z(\mathbf{z})$ (sound speed vs. depth).

## III. Estimating Source to Receiver Reflection Path Travel Time (Forward Problem)

### A. Problem Definition

The "forward problem" associated with analyzing reflection data is defined as estimating the source to receiver reflection path travel time for a given measurement geometry and $V_Z(\mathbf{z})$. A sample measurement geometry is shown in Figure 3. In this case (Fig. 3), the forward problem is to estimate the source to receiver reflection path travel time as a function of source to receiver horizontal "offset" distance $x$. The travel time as a function of $x$, $T(x)$, is commonly labeled "moveout".

Computing $T(x)$ for a geometry consisting of a single constant sound speed layer, as shown in Figure 4a, is quite simple and results in the hyperbolic "moveout" $T(x)$ as shown below and in Figure 4b.

$$T(x) = (T^2(0) + x^2/V_c^2)^{\frac{1}{2}}$$

where $x \triangleq$ source to receiver horizontal offset,

$V_c \triangleq$ sound speed in layer (constant in this case) and

$T(0) =$ Normal incidence reflection path travel time.

3

$V_z$

$V_z(z) = V_0 + gz$ (CONSTANT GRADIENT)

$V_z(z) = V_c$ (CONSTANT SPEED)

REFLECTING BOUNDARY OF INTEREST

$V_0$

RECEIVER

REFLECTION PATH

X

SOURCE

0

$D_1$

$D_2$

z

Figure 3.  Sample Geometry and Sound Speed Profile

4

SOURCE       RECEIVER

$V_z (z) = V_c$ (CONSTANT)

REFLECTION PATH
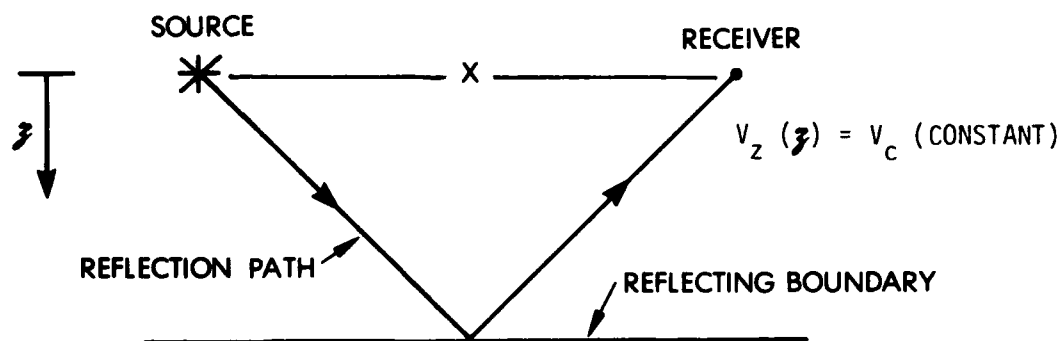
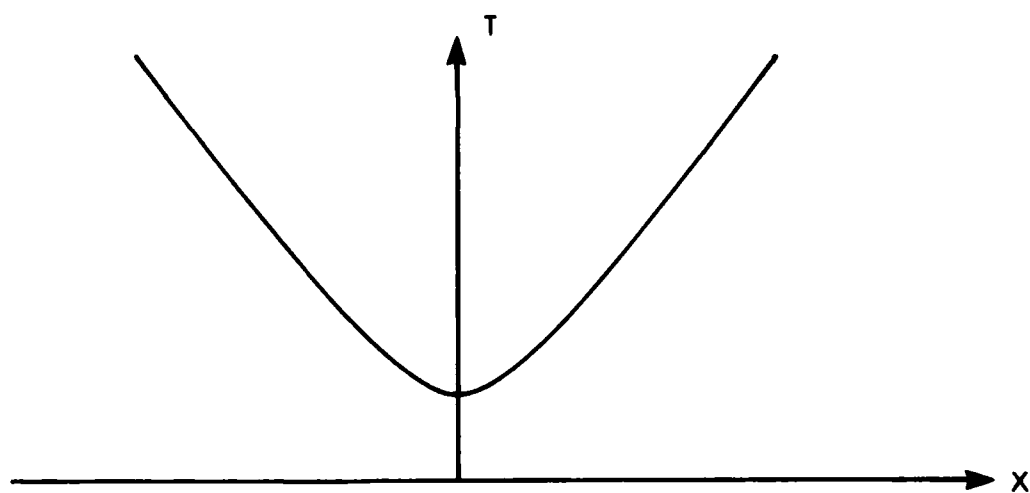REFLECTING BOUNDARY

Figure 4a. Single Constant Sound Speed Layer



Figure 4b. T(x) for Single Constant Sound Speed Layer

Computing $T(x)$ for a general $V_Z(z)$ is much more difficult. The most straightforward approach for computing $T(x)$ for a general $V_Z(z)$ is the ray trace technique, which approximates $V_Z(z)$ by a series of simple functions and then incorporates Snell's law to determine an approximate travel time and distance as a function of sound ray departure angle. Error in the approximation can be made small at the expense of computational burden by increasing the number of simple functions approximating $V_Z(z)$. It is precisely the computational burden associated with ray tracing that motivated development of the moments approach for estimating $T(x)$.

## B. Moments Approach for Estimating $T(x)$

The moments approach for estimating "moveout", $T(x)$, approximates $T(x)$ by the square root of a finite order Maclaurin series about the normal incidence reflection path, viz.

$$T(x) = (C + C x + C x + C x + C x ---)^{\frac{1}{2}} \quad (3)$$

where $x \triangleq$ source to receiver
horizontal offset and

$\quad C_i$ = function of measurement
geometry and $V_Z(z)$.

By symmetry, it is easily shown (May and Straley [1]) that odd-ordered coefficients $C_1$, $C_3$, etc., are identically zero. Deleting zero valued coefficients and squaring equation (3) results in

$$T(x) = C + C x + C x'' + C x' ------. \quad (4)$$

The series approximation is no different from that of Taner and Koehler [2] and May and Straley [1]. The moments approach differs, however, in that it addresses the *arbitrary* $V_Z(z)$ as opposed to layers of constant sound speed. A further advantage of the moments approach, which will be

discussed later, is that it lends itself more readily to the inverse problem.

Clearly the challenge associated with implementing equation (4) is determining the coefficients $C_i$. A principal feature of the moments approach is that it allows the coefficients, $C_i$, to be computed quite easily.

Coefficient $C_0$ can be related to physical conditions by evaluating equation (4) at zero offset ($x = 0$), i.e.,

$$C = T(x = 0). \quad (5)$$

Referring to the general configuration of Figure 5 leads to the following equation for $T(x=0)$.

$$T(x=0) = \int_0^{D} \frac{dz}{V_Z(z)} + \int_{D_r}^{D} \frac{dz}{V_Z(z)} \quad (6)$$

Comparing equations (6) and (1a) reveals that $T(x=0)$ and therefore $C_0$ can be expressed identically in terms of moments by

$$C = (M_{-1}) . \quad (7)$$

Differentiating equation (4) with respect to $x^2$ and taking the limit as $x$ goes to zero results in the following expression for $C_2$.

$$C = \lim_{x \to 0} \frac{dT(x)}{dx} \quad (8)$$

Evaluating $dT^2/dx^2$ in terms of physical parameters can be simplified by applying a mathematical identity to obtain

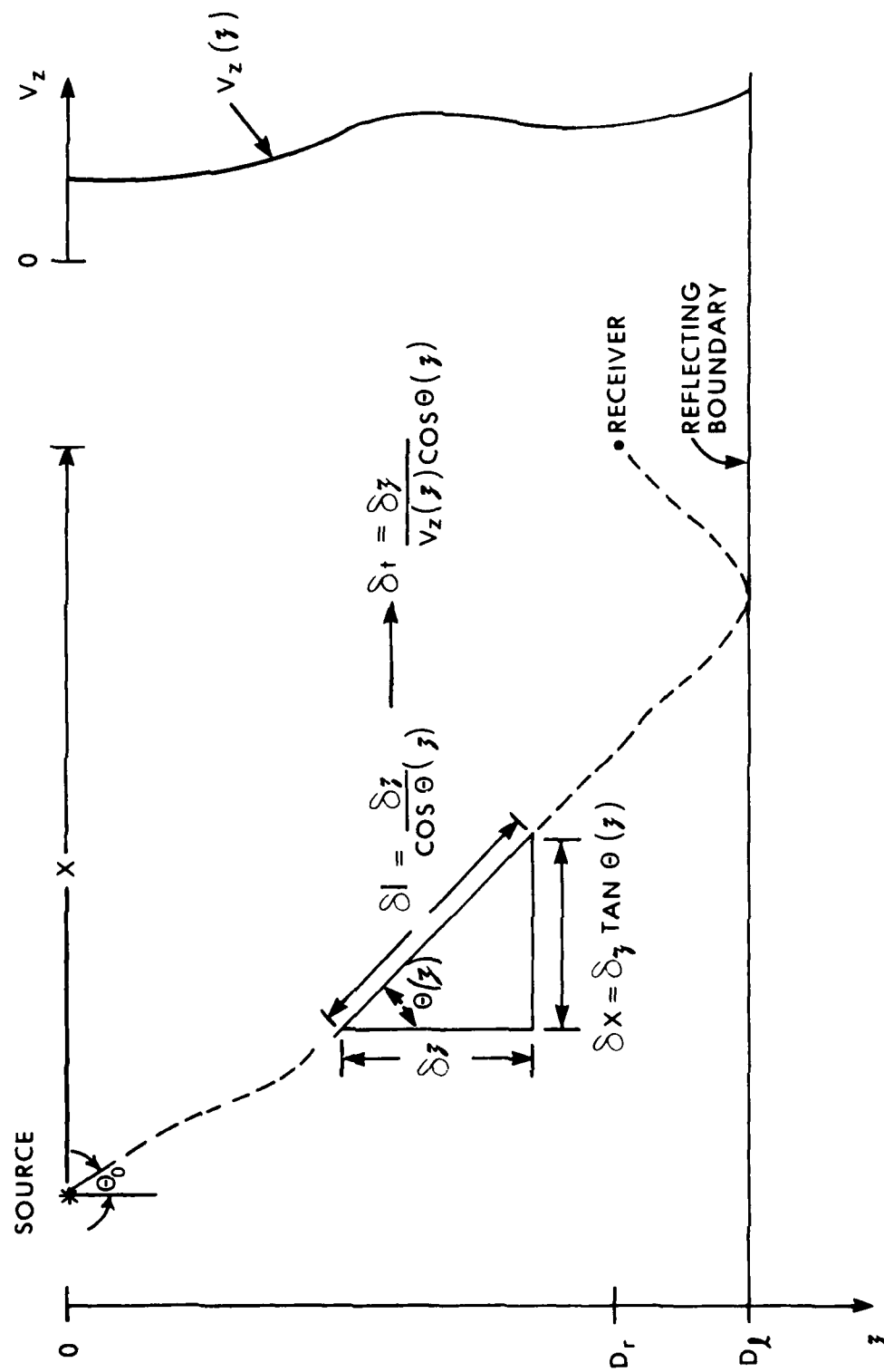$$\frac{dT}{dx} = \frac{T \, dT/dx}{x} \quad (9)$$

Figure 5. General Configuration

7

Also, $dT/dx$ can be expressed by

$$\frac{dT}{dx} = \frac{dT/d\theta_0}{dx/d\theta_0} \qquad (10)$$

Referring to the notation defined in Figure 5, expressions for x and T can be derived to yield

$$x = \int_0^{D_\ell} \tan\theta(z)\, dz \qquad (11a)$$

$$+ \int_{D_r}^{D} \tan\theta(z)\, dz \qquad \text{and}$$

$$T = \int_0^{D_\ell} \frac{dz}{V_Z(z)\cos\theta(z)} \qquad (11b)$$

$$+ \int_{D_r}^{D} \frac{dz}{V_Z(z)\cos\theta(z)}$$

where $\theta_0 \triangleq$ initial departure angle of sound ray and

$\theta(z) \triangleq$ sound ray angle at depth z for a ray departing with angle $\theta_0$.

Differentiating equations (11a) and (11b) with respect to $\theta_0$ results in

$$\frac{dx}{d\theta_0} = \int_0^{D_\ell} \frac{\frac{d\theta(z)}{d\theta_0}}{\cos^2\theta(z)}\, dz + \int_{D_r}^{D} \frac{\frac{d\theta(z)}{d\theta_0}}{\cos^2\theta(z)}\, dz \qquad (12a)$$

and

$$\frac{dT}{d\theta_0} = \int_0^{D_\ell} \frac{\sin\theta(z)\frac{d\theta(z)}{d\theta_0}}{V_Z(z)\cos^2\theta(z)}\, dz \qquad (12b)$$

$$+ \int_{D_r}^{D} \frac{\sin\theta(z)\frac{d\theta(z)}{d\theta_0}}{V_Z(z)\cos^2\theta(z)}\, dz$$

From Snell's law, the following relationships can be obtained.

$$\sin\theta(z) = \frac{V_Z(z)}{V_Z(0)}\sin\theta_0 \quad \text{and} \qquad (13a)$$

$$\frac{d\theta(z)}{d\theta_0} = \frac{V_Z(z)}{V_Z(0)}\frac{\cos\theta_0}{\cos\theta(z)} \qquad (13b)$$

Substituting equations (13) into equations (12) results in the following expressions for $dx/d\theta_0$ and $dT/d\theta_0$

$$\frac{dx}{d\theta_0} = \frac{\cos\theta_0}{V_Z(0)}\left[\int_0^{D_\ell} \frac{V_Z(z)}{\cos^3\theta(z)}\, dz + \int_{D_r}^{D} \frac{V_Z(z)}{\cos^3\theta(z)}\, dz\right]$$

$$(14a)$$

and

$$\frac{dT}{d\theta_0} = \frac{\sin\theta_0\cos\theta_0}{V_Z^2(0)}\left[\int_0^{D_\ell} \frac{V_Z(z)}{\cos^3\theta(z)}\, dz\right.$$

$$\left. + \int_{D_r}^{D_\ell} \frac{V_Z(z)}{\cos^3\theta(z)}\, dz\right] \qquad (14b)$$

Substituting equations (14) into equation (10) yields the following familiar expression (Rutherford [3]).

$$\frac{dT}{dx} = \frac{\sin\theta_0}{V_Z(0)} \qquad (15)$$

Substituting equations (13) into equation (11a) results in the following equation for x as a function of $\theta_0$.

$$x = \frac{\sin\theta_0}{V_Z(0)}\left[\int_0^{D_\ell} \frac{V_Z(z)}{\cos^2\theta(z)}\, dz + \int_{D_r}^{D} \frac{V_Z(z)}{\cos^2\theta(z)}\, dz\right] \qquad (16)$$

An expression for $dT^2/dx^2$ can now be obtained by substituting equations (16), (15), and (11b) into equation (9), viz.

$$\frac{dT^2}{dx^2} = \frac{\int_0^{D_\ell} \frac{dz}{V_z(z)\cos\theta(z)} + \int_{D_r}^{D_\ell} \frac{dz}{V_z(z)\cos\theta(z)}}{\int_0^{D_\ell} \frac{V_z(z)dz}{\cos\theta(z)} + \int_{D_r}^{D_\ell} \frac{V_z(z)dz}{\cos\theta(z)}} \quad (17)$$

To evaluate coefficient $C_2$ (equation (8)), we need the limit of $dT^2/dx^2$ as x approaches zero. Realizing that $\theta_0$ approaching zero is equivalent to x approaching zero, allows equation (17) to be evaluated in the limit to yield

$$\lim_{x \to 0} \frac{dT^2}{dx^2} = \frac{\int_0^{D_\ell} \frac{dz}{V_z^2(z)} + \int_{D_r}^{D_\ell} \frac{dz}{V_z^2(z)}}{\int_0^{D_\ell} V_z(z)dz + \int_{D_r}^{D_\ell} V_z(z)dz} \quad (18)$$

Comparing equation (18) with defining equation (1a) reveals that equation (18) and therefore coefficient $C_2$ (via equation (8)) can be expressed identically in terms of moments by

$$C_2 = \frac{M_{-1}}{M_1^2} \quad (19)$$

It is easily shown (see section IV. B.5) that $(C_2)^{-1/2}$ is identically the RMS sound speed for the normal incidence (x=0) reflection path from source to receiver, where the RMS speed, $V_{RMS}$, is defined by

$$V_{RMS} = \left[ \frac{1}{Tn} \int_0^{Tn} V_T^2(t)dt \right]^{1/2}$$

where   $Tn \triangleq$ Normal incidence reflection path travel time and

$V_T(t) \triangleq$ Sound speed as function of time.

An interesting by-product of this result is that the Dix [4] approach for determining RMS sound speed of a layer is *exact* (as opposed to approximate) for an *arbitrary* $V_z(z)$, providing that "array velocity", $V_A$, is defined as follows.

$$V_A \triangleq \lim_{x \to 0} \left( \frac{dT^2}{dx^2} \right)^{-1/2}$$

Higher order coefficients of the $T^2(x)$ polynomial are derived in Appendix B. For brevity, only the results are presented here.

$$C_2 = (M_{-1}) \quad (20a)$$

$$C_2 = \frac{M_{-1}}{M_1} \quad (20b)$$

$$C_4 = \frac{1}{4M_1} \left[ 1 - \frac{M_{-1} M_3}{M_1^2} \right] \quad (20c)$$

$$C_6 = \frac{1}{8M_1^3} \left[ \frac{2 M_4 M_{-1}}{M_1} - M_1 M_2 - M_5 M_{-1} \right] \quad (20d)$$

$$C_8 = \frac{1}{64M_1^5} \left[ 9 M_4 M_1 + 24 M_3 M_5 M_{-1} - \frac{24 M_2 M_{-1}}{M_1} \right.$$
$$\left. - 4 M_6 M_1^2 - 5 M_7 M_{-1} M_1 \right] \quad (20e)$$

The technique presented in Appendix B can be used to derive higher order coefficients ($C_{10}$, etc.). Practical experience, however, has indicated that an eighth order "moveout" $T^2(x)$ polynomial is more than adequate to obtain accuracy comparable to a practical ray trace algorithm.

The important feature of this derivation is that the finite order $T^2(x)$ polynomial can be generated easily using the moments approach for virtually *any* $V_Z(z)$ of interest.

## C. Accuracy of the Moments Approach for Estimating T(x)

Accuracy of the moments approach for estimating reflection path "moveout" was investigated by comparing $T(x)$ computed from the moments approach, $T_M(x)$, with that computed from a standard ray trace algorithm, $T_R(x)$. Experiments were conducted for a variety of sound speed profiles, a few of which are presented here.

The first experiment considers a single 200 m thick layer with a sound speed gradient of 1.5 sec$^{-1}$. Figure 6a displays the measurement configuration and sound speed profile. Figure 6b displays the error (difference between ray trace and moments approach) as a function of source to receiver horizontal offset x. Errors for the second order through eighth order moments approach are presented. Notice that an eighth order approximation estimates $T(x)$ to within 2 microseconds.

The second experiment involves a more detailed sound speed profile as shown in Figure 7a. Performance of the moments approach is illustrated in Figure 7b.

The third experiment is designed to show *versatility* and *computational savings* offered by the moments approach for handling a more general $V_Z(z)$. A quadratic sound speed versus depth relationship, as shown in Figure 8a, is considered. In order to implement the ray trace algorithm, it was necessary to *approximate* the quadratic $V_Z(z)$ by a set of N linear sound speed versus depth relationships. Accuracy of the ray trace algorithm improves, of course, with increasing N. Figure 8b displays the difference (T(x) estimates) between ray trace and the eighth order moments approach as a function of

N for a source to receiver offset of 950 m. Notice that as N becomes large, the ray trace estimate, $T_R$, converges near the moments approach estimate. Computational savings offered by the moments approach over ray trace for N=100 is approximately two orders of magnitude.*

## IV. Estimating $V_Z(z)$ from Reflection Data (Inverse Problem)

### A. Problem Definition

The "inverse problem" of estimating a sound speed versus depth relationship from acoustic reflection travel time data is considerably more difficult than the forward problem. The level of difficulty increases with generality of the solution. As an example, the Dix [4] approach for estimating RMS sound speed of a layer is quite simple, whereas estimating a linear sound speed versus depth relationship (Gibson, Odegard and Sutton [5]) can be orders of magnitude more difficult. The Dix approach, therefore, features simplicity at the expense of only estimating RMS sound speed (1 parameter) of the layer of interest. The technique used by Gibson et al. [5] features more generality (linear sound speed versus depth relationship) at the expense of additional computational burden. The particular approach used by Gibson et al. [5] uses a ray trace technique coupled with a nonlinear estimation algorithm to determine layer characteristics (thickness, gradient, etc.) necessary to *match* the observed moveout, $T(x)$. The moments approach inversion technique presented in this report features generality (linear sound speed versus depth relationship) with only a slight increase in computational burden.

---

*Actual results, using available software, indicated a 400 to 1 time reduction in computational burden using the moments approach.
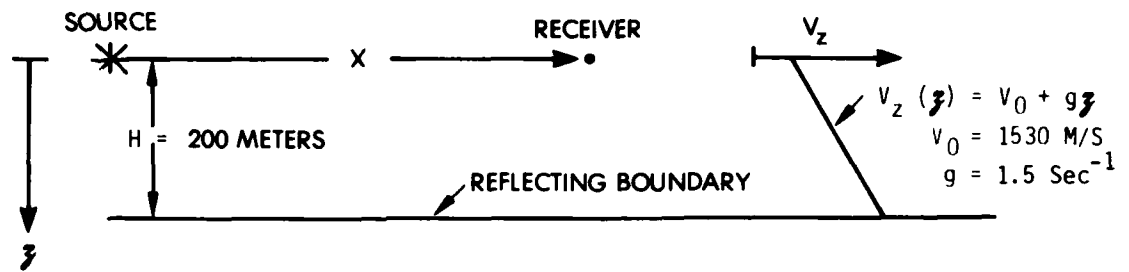
10

Figure 6a. Measurement Configuration and Sound Speed Versus Depth Relationship
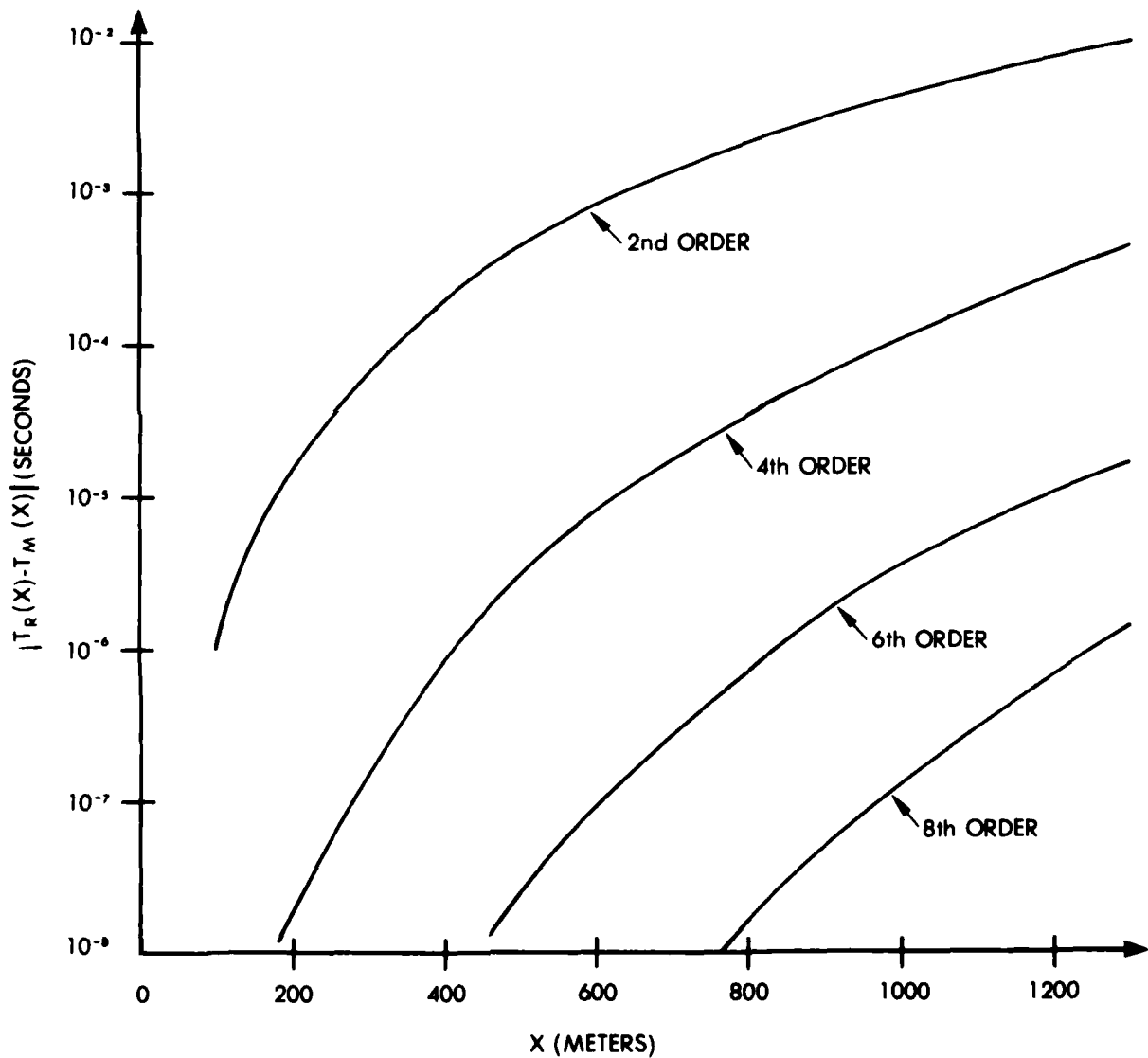


Figure 6b. Errors in T(x) Computed from Moments Approach
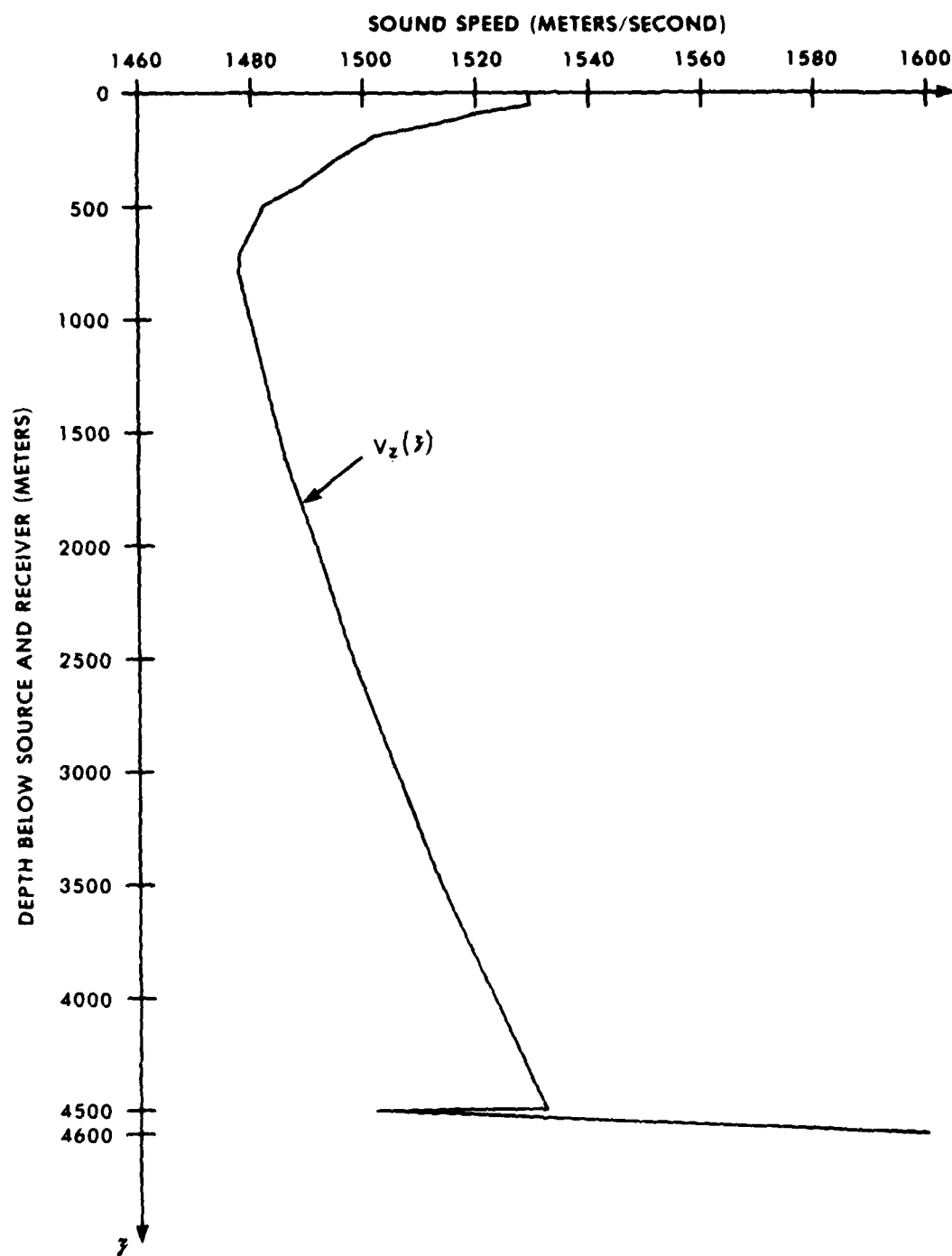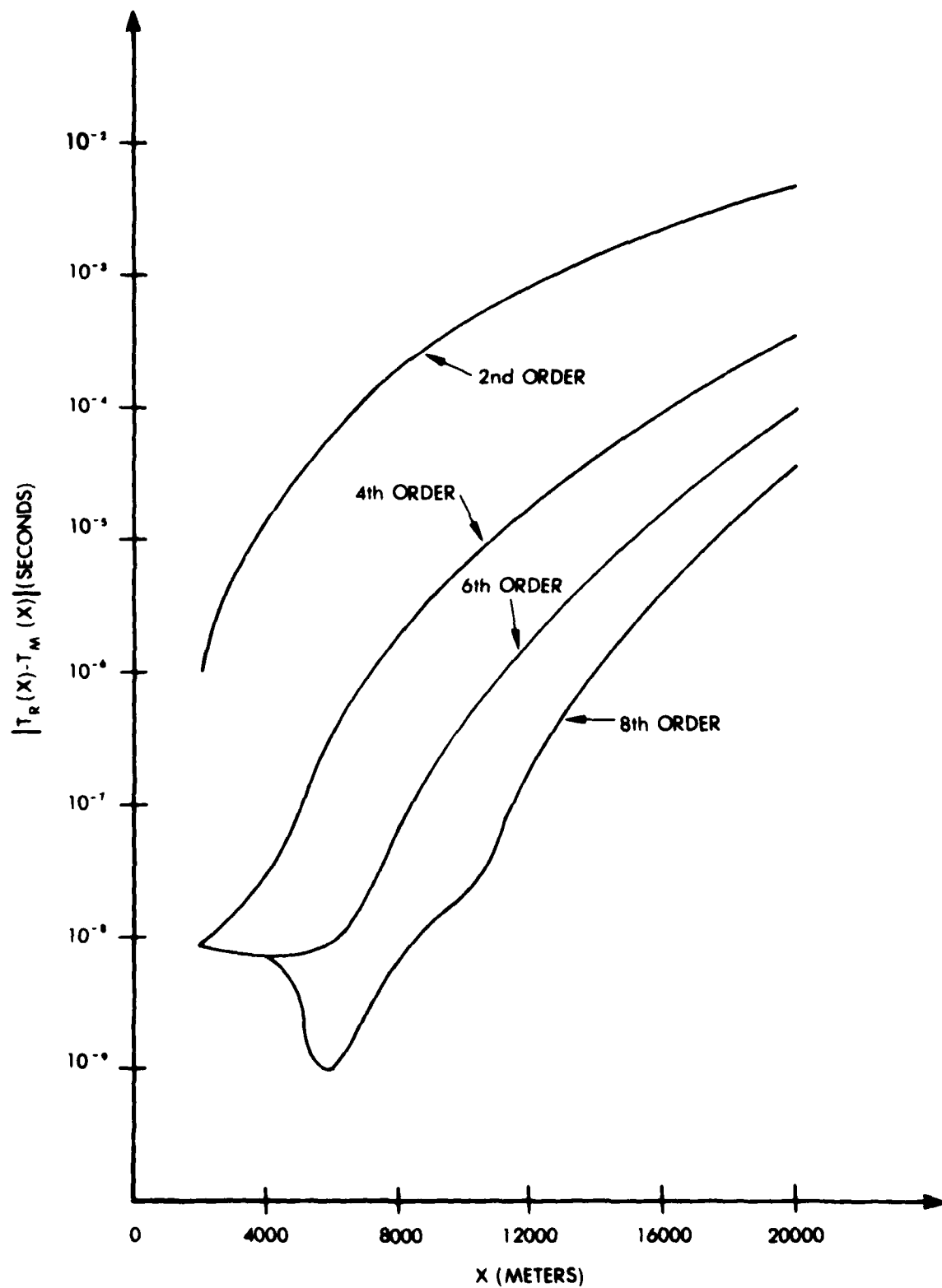
Figure 7a. Sound Speed Profile
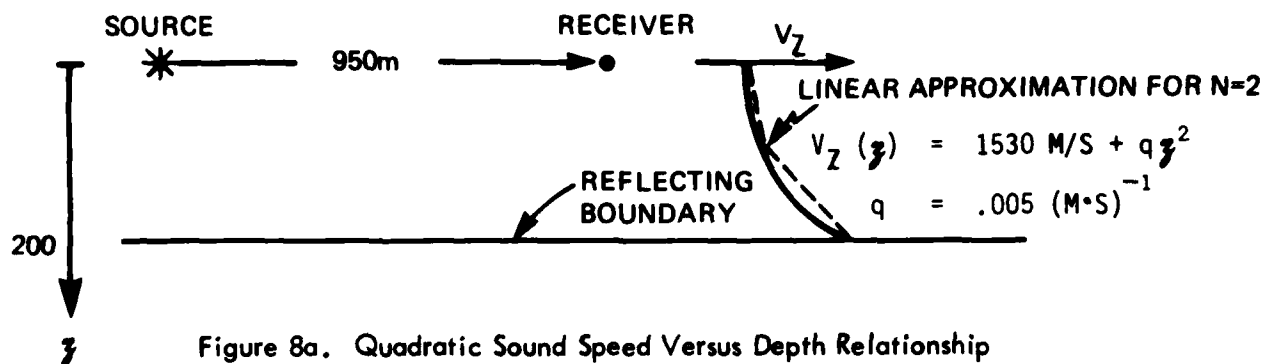
Figure 7b. Errors in T(x) Computed From Moments Approach

13

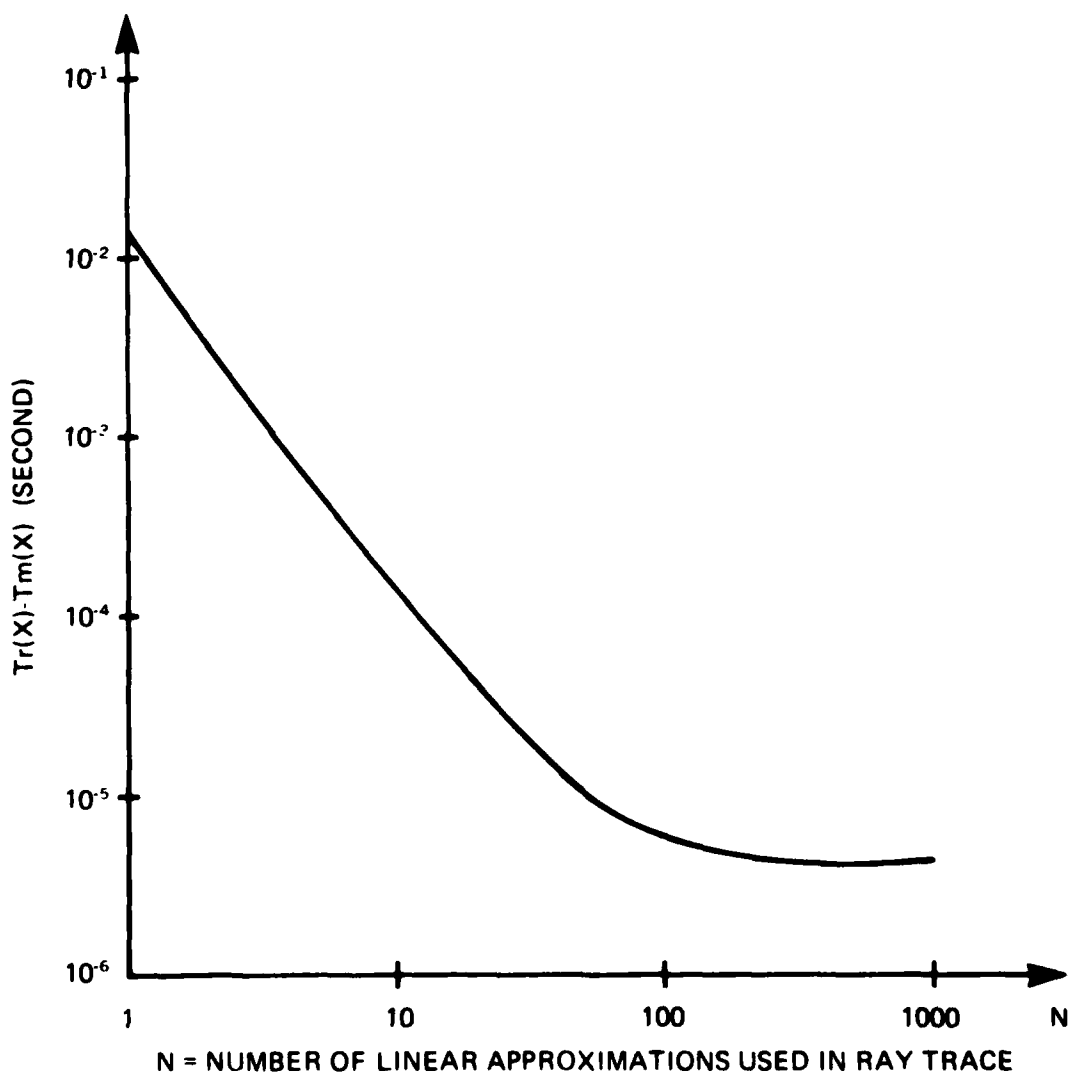Figure 8a.  Quadratic Sound Speed Versus Depth Relationship



Figure 8b.  Difference Between Ray Trace and Moments Approach

14

## B. Moments Approach for Estimating a Linear Sound Speed Versus Depth Relationship (Single Layer Case)

The moments approach offers a very simple technique for estimating a linear sound speed versus depth relationship from acoustic reflection data. Specifically, the approach estimates the following parameters describing the layer of interest.

o Thickness (H)
o Sound speed at "top" of the layer ($V_T$)
o Sound speed at "bottom" of the layer ($V_B$)
o Sound speed gradient, $dV_z/dz$, (g)
o RMS sound speed ($V_{RMS}$)

For simplicity, the algorithm will be first derived for a *single layer case*. Also, for simplicity, the algorithm is derived for the case where source and receiver (or an array of receivers) are at the same depth. Measurement geometry and $V_z(z)$ for the single layer case are shown in Figure 9. The source and receiver (or array of receivers) is used to measure the *reflection path travel time* T(x) where x is the source to receiver horizontal offset.

The procedure for estimating layer parameters from measured T(x) (denoted by $T_{meas}(x)$) is very much the reverse of estimating T(x) from known layer parameters. More specifically, the procedure follows in steps as outlined below.

Step 1: Relate moveout polynomial coefficients, $C_i$, to measured travel time data.

Step 2: Relate moments, $M_i$, to coefficients $C_i$.

Step 3: Relate layer parameters, H, $V_T$, etc., to moments.

### 1. Step 1 (Determine Polynomial Coefficients)

The *first step* is simply "fitting" a polynomial to the measured moveout squared, $T^2_{meas}(x)$. Performing this step results in a polynomial expression as shown below,

$$T^2_{meas}(x) = C_0 + C_2 x^2 + C_4 x^4 + C_6 x^6 \ldots$$

where $T_{meas}(x) \triangleq$ Measured reflection path travel time as a function of source to receiver horizontal offset, x.

Many techniques (least squares etc.) exist for determining the coefficients, $C_i$. Details of these techniques will not be described here. For a linear sound speed versus depth relationship, only coefficients $C_0$, $C_2$ and $C_4$ are needed.

### 2. Step 2 (Compute Moments)

The *second step* relates moments of the sound speed profile to coefficients, $C_i$, determined in step 1. For a linear sound speed versus depth relationship, only moments $M_{-1}$, $M_1$ and $M_3$ need be computed. Equations (20) can be solved to yield the following expressions for relating moments to polynomial coefficients.

$$M_{-1} = (C_0)^{1/2}$$

$$M_1 = \frac{C_0^{1/2}}{C_2}$$

$$M_3 = \left(\frac{C_0^{1/2}}{C_2}\right)\left(1 - 4C_4 \frac{C_0}{C_2}\right)$$

### 3. Step 3 (Closed Form Approximate Solution)

The *third step*, relating layer parameters to moments, is somewhat more difficult. Relating moments to layer parameters, for a linear sound speed versus depth relationship, using equation (1b) results in the following.

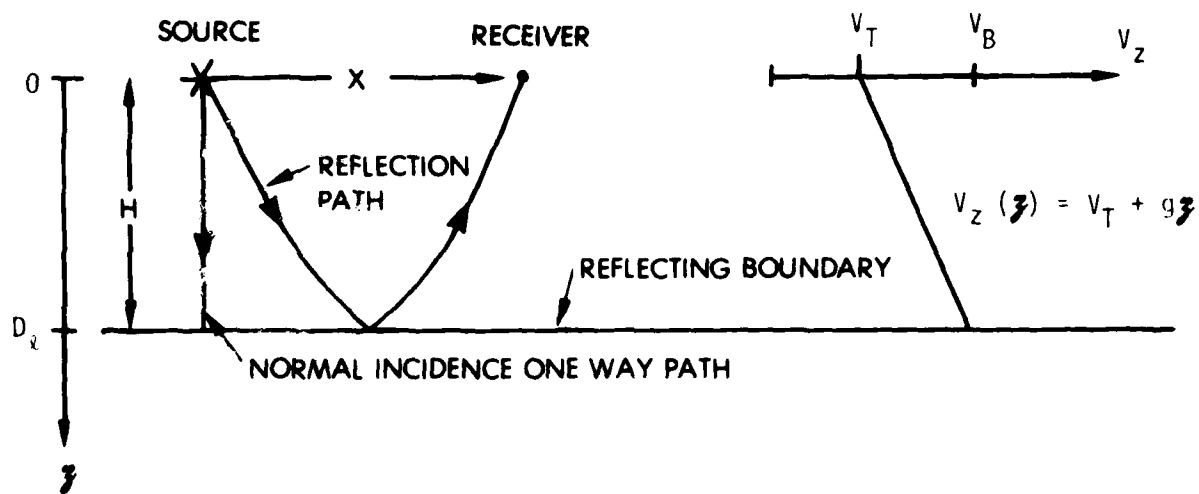$$M_{-1} = \frac{2}{g} \ln \left[\frac{V_B}{V_T}\right] \qquad (21a)$$

15

Figure 9. Single Layer with Linear Sound Speed Versus Depth Relationship

$$V_z(z) = V_T + gz$$

16

$$M_1 = \frac{1}{g} (V_B^2 - V_T^2) \tag{21b}$$

$$M_3 = \frac{1}{2g} (V_B^4 - V_T^4) \tag{21c}$$

where $V_T \overset{\Delta}{=}$ Sound speed at "top" of the layer,

$V_B \overset{\Delta}{=}$ Sound speed at "bottom" of the layer,

$g \overset{\Delta}{=}$ Sound speed gradient and

$\ln(.)$ denotes natural logarithm.

Substituting for g ($g = (V_B - V_T)/H$) where H is the layer thickness, results in a more convenient form.

$$M_{-1} = \frac{2H}{V_B - V_T} \ln \left( \frac{V_B}{V_T} \right) \tag{22a}$$

$$M_1 = (V_T + V_B)H \tag{22b}$$

$$M_3 = \frac{(V_T + V_B)(V_T^2 + V_B^2)H}{2} \tag{22c}$$

Inverting equations (22) to find layer parameters as a function of moments, involves the solution of nonlinear algebraic equations. Unfortunately, no closed form solution has been found. A *closed form approximate* solution can be obtained, however, by expanding the natural log function of equation (22a) about $V_T/V_B = 1$ (Ref. [6]). Performing this expansion, and introducing a correction factor, $\eta$, results in the following representation for equation (22a).

$$M_{-1} = \frac{4\eta H}{V_T + V_B} \tag{23}$$

The correction factor, $\eta$, is given by

$$\eta = \frac{\ln \left( \frac{V_B}{V_T} \right) (V_T + V_B)}{2 (V_B - V_T)} \tag{24}$$

Unfortunately, equation (24) involves the *unknown* parameters $V_T$ and $V_B$. Equation (24) will be used, however, in the *iterative* solution presented in the next section. For <u>practical cases</u>, $\eta$ <u>will be very nearly unity</u>.

Equations (23), (22b) and (22c) can be solved in closed form to yield the following expressions relating layer parameter estimates ($\hat{H}$, etc.) to moments.

$$\hat{H} (\eta) = \left( \frac{M_1 M_{-1}}{4\eta} \right)^{\frac{1}{2}}$$

$$\hat{V}_T (\eta) = \frac{M_1 - Q}{2\hat{H}}$$

$$\hat{V}_B (\eta) = \frac{M_1 + Q}{2\hat{H}}$$

where $Q \overset{\Delta}{=} K \left( \frac{M_3 M_{-1}}{\eta} - M_1^2 \right)^{\frac{1}{2}}$

$K = \pm 1$ (See Section B.6, page 20)

The closed form approximate solution assumes $\eta$ is identically unity. With this assumption, the closed form approximate solution becomes

$$\hat{H} = \left( \frac{M_1 M_{-1}}{4} \right)^{\frac{1}{2}} \tag{25a}$$

$$\hat{V}_T = \frac{M_1 - Q}{2\hat{H}} \tag{25b}$$

$$\hat{V}_B = \frac{M_1 + Q}{2\hat{H}} \tag{25c}$$

where $Q \overset{\Delta}{=} K (M_3 M_{-1} - M_1^2)^{\frac{1}{2}}$ and

$K = \pm 1$ (See Section B.6, page 20)

4. **Step 3 (Iterative Solution)**

For many applications, the closed form approximate solution of equations (25) provides acceptable results. If greater accuracy is desired, the *iterative* solution described in Figure 10 can be used.

17

Block 1:
$$n = 1$$
$$K = \pm 1 \text{ (Section B.6)}$$

Block 2:
$$\hat{H} = \left(\frac{M_1 \, M_{-1}}{4n}\right)^{\frac{1}{2}}$$

$$Q = K \left(\frac{M_3 \, M_{-1}}{n} - M_1^{\;2}\right)^{\frac{1}{2}}$$

$$\hat{V}_T = \frac{M_1 - Q}{2\hat{H}}$$

$$\hat{V}_B = \frac{M_1 + Q}{2\hat{H}}$$

Block 3:
$$n = \frac{\ell n\left(\dfrac{\hat{V}_B}{\hat{V}_T}\right)\left(\hat{V}_T + \hat{V}_B\right)}{2\left(\hat{V}_B - \hat{V}_T\right)}$$
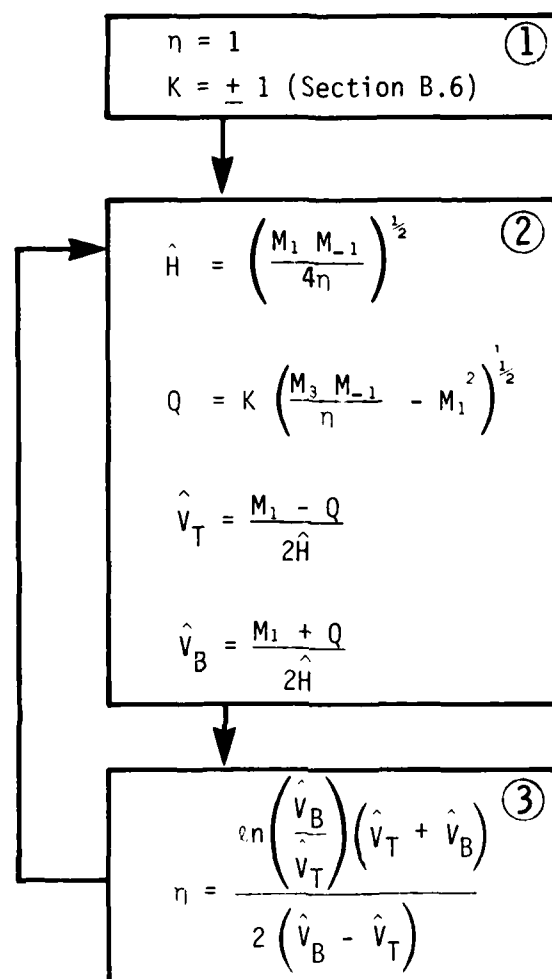
Figure 10. Iterative Solution

The "loop" from Block ③ to Block ② of Figure 10 is repeated until estimates for $\hat{V}_T$, $\hat{V}_B$, and $\hat{H}$ converge.

As an example, consider a layer described by the following parameters.

$H = 100$ m
$V_T = 1500$ m/sec
$V_B = 1600$ m/sec

Table 1 illustrates properties of the iterative solution by tabulating $\hat{H}$, $\hat{V}_T$, and $\hat{V}_B$ as a function of the number of iterations. Results of the <u>closed form approximate</u> solution are shown as zero iterations.

### 5. Estimating Gradient and RMS Sound Speed

Once $\hat{V}_T$, $\hat{V}_B$ and $\hat{H}$ are determined, an estimate of sound speed gradient follows directly from the definition of gradient for a constant gradient layer, i.e.,

$$\hat{g} = (\hat{V}_B - \hat{V}_T)/\hat{H} \tag{26}$$

The RMS sound speed, $V_{RMS}$, of the layer is defined as the root-mean-square speed of a sound ray travelling at normal incidence, i.e.,

$$V_{RMS} \triangleq \left( \frac{1}{T_\ell} \int_0^{T_\ell} V_T^2 (t)\, dt \right)^{1/2} \tag{27}$$

where $T_\ell$ = Normal incidence (one way) travel time from $z=0$ to $z=D_\ell$ of Figure 9 and

$V_T(t) \triangleq$ Speed of a sound ray traveling at normal incidence as a function of <u>time</u>, t.

Rearranging the integration of equation (27) allows $V_{RMS}$ to be expressed by

$$V_{RMS} = \left( \frac{1}{T_\ell} \int_0^{D_\ell} V_T^2 (t(z))\, d\,(t(z)) \right)^{1/2} \tag{28}$$

The function $V_T(t(z))$ is, of course, identically $V_Z(z)$.

$$V_T(t(z)) \equiv V_Z(z) \tag{29}$$

Also the function $t(z)$ can be expressed by

$$t(z) = \int_0^z \frac{dy}{V_Z(y)} \tag{30}$$

Differentiating equation (30) with respect to $z$ and solving for the differential $d(t(z))$ results in

$$d(t(z)) = \frac{dz}{V_Z(z)} \tag{31}$$

Table 1. Example of Closed Form Approximate and Iterative Solution (Single Layer Case)

| Number of Iterations | | $\hat{H}$ (m) | $\hat{V}_T$ (m/sec) | $\hat{V}_B$ (m/sec) |
|---|---|---|---|---|
| 0 | (Closed form approx. solution) | 100.017 | 1491.994 | 1607.468 |
| 1 | | 99.994 | 1502.958 | 1597.222 |
| 2 | | 100.002 | 1499.048 | 1600.892 |
| 3 | | 99.999 | 1500.322 | 1599.698 |
| 4 | | 100.000 | 1499.893 | 1600.100 |

Substituting equations (31) and (29) into equation (28) results in the following expression for $V_{RMS}$.

$$V_{RMS} = \left( \frac{1}{T_\ell} \int_0^{D_\ell} V_z(z)\,dz \right)^{\frac{1}{2}} \tag{32a}$$

Relating equation (32a) to moments yields

$$V_{RMS} = \left( \frac{M_1/2}{M_{-1}/2} \right)^{\frac{1}{2}}$$

which is identically $(C_2)^{\frac{1}{2}}$.

Therefore, an estimate of RMS sound speed of the layer can be obtained immediately after Step 1, viz.

$$V_{RMS} = (C_2)^{-\frac{1}{2}} \tag{32b}$$

where $C_2$ is a coefficient in the moveout polynomial. Equation (32b) is true for any sound speed versus depth relationship, whereas Equation (26) is true only for a constant gradient case.

## 6. Ambiguity

An unfortunate ambiguity exists when "inverting" reflection path travel time data from a constant gradient layer. To explain the ambiguity, equations for moments of a constant gradient layer are repeated here.

$$M_{-1} = \frac{2}{g} \ln \left[ \frac{V_B}{V_T} \right] \tag{33a}$$

$$M_i = \frac{2}{(i+1)g} \left[ V_B^{i+1} - V_T^{i+1} \right] \quad i \neq -1 \tag{33b}$$

where $V_T \triangleq$ Sound speed at "top" of layer and

$V_B \triangleq$ Sound speed at "bottom" of layer

Notice from equations (33) that if $V_T$ and $V_B$ are interchanged (g becomes $-g$) the moments, $M_i$, *remain unchanged*. Consequently, the moveout, $T(x)$, for reflection path data, is not a function of the polarity of the sound speed gradient. Therefore, successful "inversion" depends on a priori knowledge of the polarity of sound speed gradients in constant gradient layers. In view of this, the rules for picking K of equations (25) and Figure 10 become

K = +1 For sound speed increasing with increasing depth and

K = −1 For sound speed decreasing with increasing depth.

## 7. Summary (Single Layer Case)

For clarity, the procedure for estimating a linear sound speed versus depth relationship from reflection path travel time data is summarized here.

Step 1: Fit polynomial to measured moveout data $T_{meas}(x)$ to obtain coefficients, $C_i$, of the moveout polynomial

$$T_{meas}(x) = C_0 + C_2 x^2 + C_4 x^4 + C_6 x^6 \ldots$$

Step 2: Compute moments from moveout polynomial coefficients.

$$M_{-1} = (C_0)^{\frac{1}{2}}$$

$$M_1 = \frac{C_2^{\frac{1}{2}}}{C_2}$$

$$M_2 = \left( \frac{C_0^{\frac{1}{2}}}{C_2^2} \right) \left( 1 - 4C_4 \frac{C_0}{C_2^2} \right)$$

20

**Step 3 (Closed Form Approximate Solution):** Compute estimates of layer parameters from moments.

$$\hat{H} = \left(\frac{M_1 M_{-1}}{4}\right)^{\frac{1}{2}}$$

$$\hat{V}_T = \frac{M_1 - Q}{2H}$$

$$\hat{V}_B = \frac{M + Q}{2H}$$

where $Q = K(M_1 M_{-1} - M_1^2)^{\frac{1}{2}}$

$K = +1$ for sound speed <u>increas-ing</u> with increasing depth

$K = -1$ for sound speed <u>decreas-ing</u> with increasing depth

**Step 3 (Iterative Solution):** To improve accuracy of Step 3, the itera-tive solution described in Figure 10 may be used.

<u>Estimating gradient and RMS sound speed</u> is performed very simply by:

$$g = (\hat{V}_B - \hat{V}_T)/H$$

$$\hat{V}_{RMS} = (C)^{-\frac{1}{2}}$$

## C. Moments Approach for Estimating a Linear Sound Speed Versus Depth Relationship (Multilayer Case)

Extending the moments approach to estimate a linear sound speed versus depth relationship for the multilayer case is reasonably simple. Basically, the extension involves processing *two* measured moveouts, $T(x)$, to determine moments for the layer of interest.

Figure 11 illustrates the general meas-urement configuration and a multilayer sound speed profile. Moveout data for the upper reflecting boundary, $Tu(x)$, and lower reflecting boundary, $T_\ell(x)$, are used to compute moments, $M_i$, of the layer of interest. The moments, $M_i$, are then used to estimate layer parameters by incorporating the *single layer procedure* derived in previous sections.

The procedure for estimating layer parameters of interest follows in steps and is described below.

1. **Step 1 (Determine "Upper" Moments)**

Observe moveout, $Tu_{meas}(x)$, of the reflection path associated with the *upper* reflecting boundary (see Fig. 11). Compute polynomial coefficients, $Cu_i$, describing measured moveout to satisfy

$$Tu_{meas}(x) = Cu_0 + Cu_1 x + Cu_2 x^2 + Cu_3 x^3 \ldots$$

Compute "upper" moments, $Mu_i$, from coefficients $Cu_i$. As in the single layer case, only 3 moments are required for the linear sound speed versus depth relationship.

$$Mu_{-1} = (Cu_0)^{\frac{1}{2}} \tag{34a}$$

$$Mu_1 = \frac{Cu_1^{\frac{1}{2}}}{Cu_2} \tag{34b}$$

$$Mu = \left(\frac{Cu_0^{\frac{1}{2}}}{Cu_2}\right)\left(1 - 4 Cu_0 \frac{Cu}{Cu_2}\right) \tag{34c}$$

2. **Step 2 (Determine "Lower" Moments)**

Observe moveout, $T\ell_{meas}(x)$, of the reflection path associated with the *lower* reflecting boundary (see Fig. 11). Compute polynomial coefficients, $C\ell_i$, describing measured moveout to satisfy

$$T\ell_{meas}(x) = C_0 + C_1 x + C_2 x^2 + C_3 x^3 \ldots$$

Compute "lower" moments, $M\ell_i$, from coefficients $C\ell_i$.
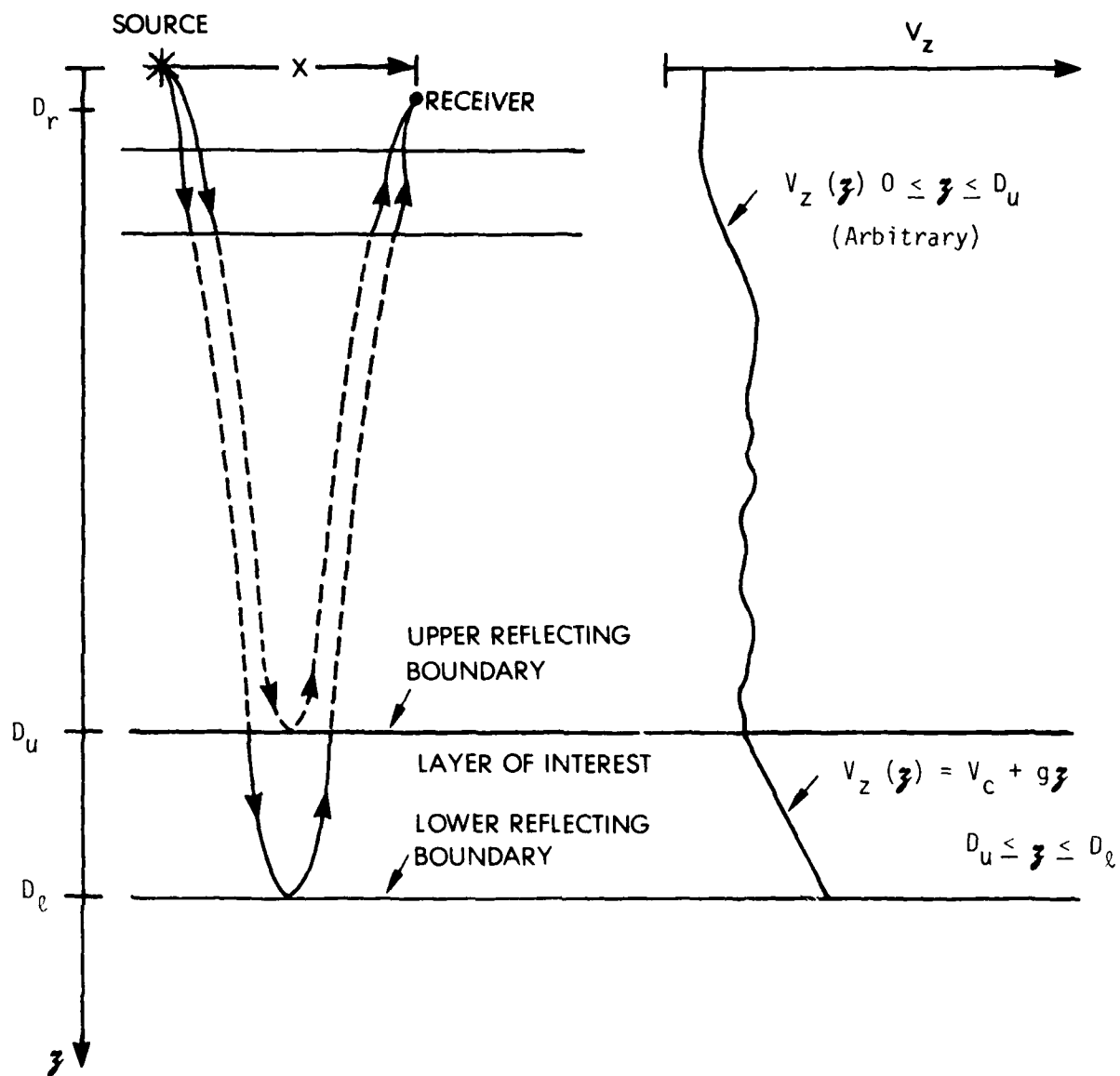
$$M\ell_{-1} = (C\ell_0)^{\frac{1}{2}} \tag{35a}$$

21

Figure 11.  Multilayer Sound Speed Profile (General Model)

$$M\ell_1 = \frac{C\ell_0^{\frac{1}{2}}}{C\ell_2} \qquad (35b)$$

$$M\ell_3 = \left(\frac{C\ell_0^{\frac{1}{2}}}{C\ell_2^2}\right)\left(1 - 4C\ell_4 \frac{C\ell_0}{C\ell_2^2}\right) \qquad (35c)$$

## 3. Step 3 (Compute Moments)

Compute moments, $M_i$, for the <u>layer of interest</u> using the upper and lower moments.

$$M_i = M\ell_i - Mu_i \quad i = -1,1,3 \qquad (36)$$

## 4. Step 4 (Closed Form Approximate Solution)

Relate layer parameters of interest to moments computed from step 3.

$$\dot{H} = \left(\frac{M_1 M_{-1}}{4}\right)^{\frac{1}{2}} \qquad (37a)$$

$$\dot{V}_T = \frac{M_1 - Q}{2\dot{H}} \qquad (37b)$$

$$\dot{V}_B = \frac{M_1 + Q}{2\dot{H}} \qquad (37c)$$

$$\dot{g} = (\dot{V}_B - \dot{V}_T) / \dot{H} \qquad (38)$$

$$\dot{V}_{RMS} = \left(\frac{M_1}{M_{-1}}\right)^{\frac{1}{2}} \qquad (39)$$

where

$$Q = K (M_3 M_{-1} - M_1^2)^{\frac{1}{2}}$$

K = +1 for sound speed <u>increasing</u> with increasing depth

K = -1 for sound speed <u>decreasing</u> with increasing depth

## 5. Step 4 (Iterative Solution)

In many cases, the closed form approximate solution of equations (37) is accurate enough. If better accuracy is desired, the iterative solution of Figure 10 can be incorporated. In either case (closed form approximate or iterative) estimates of sound speed gradient, g, and RMS sound speed, $V_{RMS}$, are given by equations (38) and (39).

## 6. Derivation of Step 3

Steps 1, 2 and 4 are essentially identical to their single layer case counterparts and therefore will not be discussed further.

Step 3, specifically equation (36), will now be derived. The moments of interest describe the layer of interest and are therefore defined by

$$M_i = 2 \int_{D_u}^{D_\ell} V_Z^i(z) dz \qquad (40)$$

where $D_u$ and $D\ell$ are depths of the upper and lower reflecting boundaries (see Fig. 11). The "upper" moments, $Mu_i$, computed in step 1 describe $V_Z(z)$ for $0 \le z \le D_u$. The "lower" moments, $M\ell_i$, computed in step 2 describe $V_Z(z)$ for $0 \le z \le D\ell$. Therefore, $Mu_i$ and $M\ell_i$ represent the following information.

$$Mu_i = \int_0^{D_u} V_Z^i(z) dz + \int_{D_r}^{D_u} V_Z^i(z) dz \qquad (41a)$$

$$M\ell_i = \int_0^{D_r} V_Z^i(z) dz + \int_{D_r}^{D_\ell} V_Z^i(z) dz \qquad (41b)$$

Subtracting equation (41a) from (41b) therefore results in the moment of interest, i.e.,

$$M_i = M\ell_i - Mu_i \qquad (42)$$

## 7. Multilayer Example

Figure 12 displays an example measurement system geometry and multilayer sound speed profile. The layer of interest is described by

$$H = 60 \text{ m},$$

$$V_T = 1560 \text{ m/sec, and}$$

$$V_B = 1650 \text{ m/sec}.$$

Steps 1, 2 and 3 were executed to obtain three moments ($M_{-1}$, $M_1$, $M_3$) for the layer of interest. Step 4 was executed to obtain the closed form approximate and iterative solution for layer parameters. Results of step 4 are displayed in Table 2. Results of the closed form approximate solution are displayed as 0 iterations.

## 8. Features of the Solution

Notice from the derivations that computations for $M_i$ depend only on move-out data from reflecting boundaries directly above and below the layer of interest. Therefore, the moments approach for estimating a linear sound speed versus depth relationship is similar to the Dix |4| approach for estimating RMS sound speed. The significance of this similarity is that only errors (measurement or otherwise) associated with two sets of measurement data *influence the parameter estimates* for the layer of interest.

Also notice that while a *linear* sound speed versus depth relationship $V_Z(z)$ is assumed for the layer of interest, *absolutely no constraining assumption* is made concerning $V_Z(z)$ outside the layer of interest.

## V. Summary and Recommendations

A "moments" approach has been developed for processing geophysical acoustic reflection data. The major feature of the moments approach is a tremendous reduction in computational burden over standard ray trace techniques. The "forward" problem of computing reflection path travel time has been solved using the moments approach for the case of an *arbitrary* sound speed versus depth relationship. The "inverse" problem of estimating a sound speed versus depth realtionship from measured reflection data has also been addressed using the moments approach. A closed form approximate solution and an iterative solution has been developed for estimating a *linear* sound speed versus depth relationship (constant gradient). The derivation makes no constraining assumption concerning the sound speed versus depth relationship *outside* the layer of interest. All derivations, forward and inverse, assume a laterally homogeneous medium with nonsloping boundaries.

Additional efforts should be directed toward extending the moments approach to sloping boundaries and perhaps laterally nonhomogeneous mediums. Also, an extension to higher order (higher than linear sound speed versus

Table 2   Example of Closed Form Approximate and Iterative Solution (Multilayer Case)

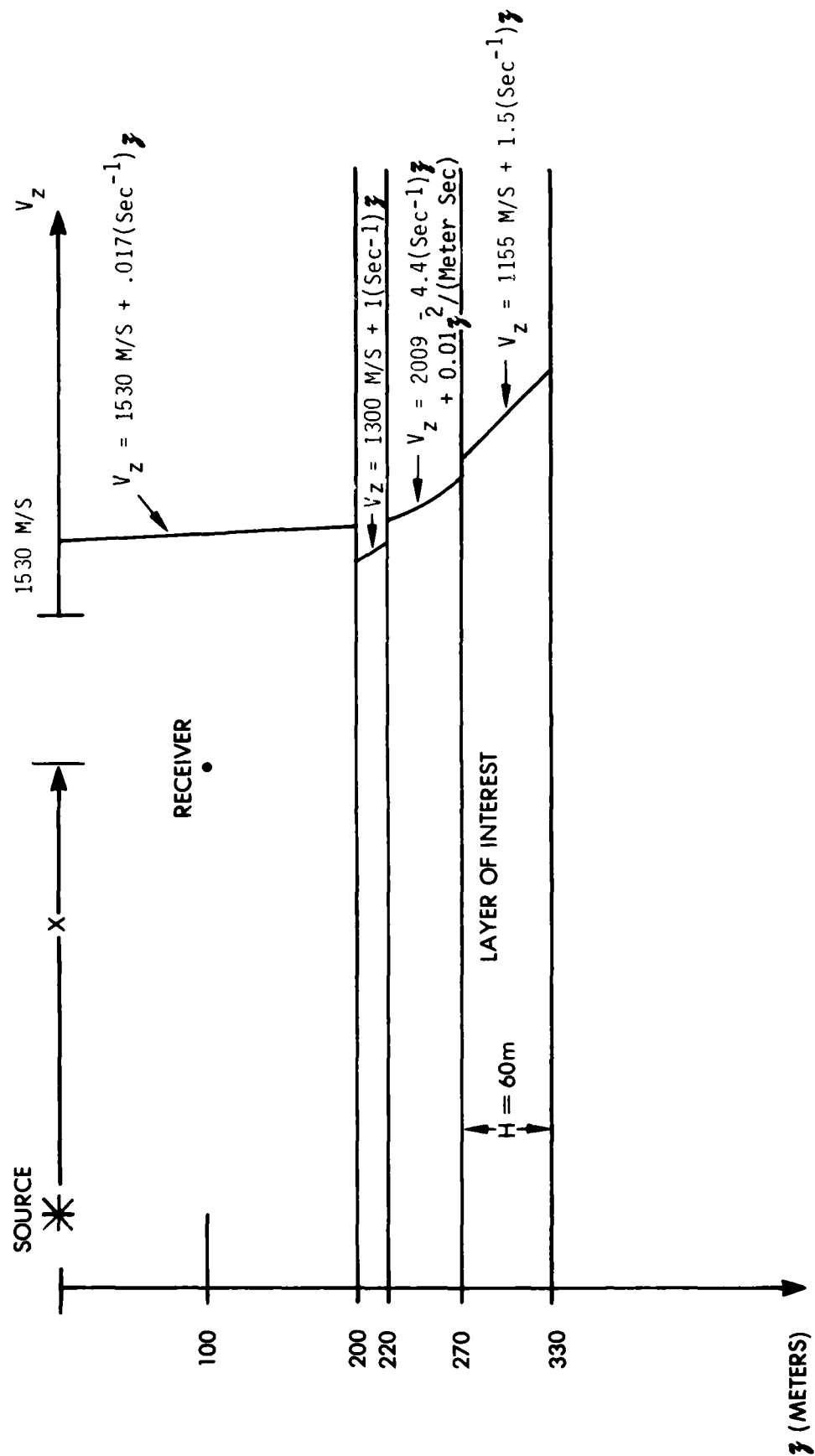| Number of Iterations | | $\hat{H}$ (m) | $\hat{V}_T$ (m/sec) | $\hat{V}_B$ (m/sec) |
|---|---|---|---|---|
| 0 | (Closed form approx. solution) | 60.008 | 1552.827 | 1656.753 |
| 1 | | 59.997 | 1562.649 | 1647.491 |
| 2 | | 60.001 | 1559.148 | 1650.805 |
| 3 | | 60.000 | 1560.288 | 1649.728 |
| 4 | | 60.000 | 1559.904 | 1650.090 |

Figure 12. Sample Multilayer Sound Speed Profile

depth relationships) inversion tech-
niques should be investigated along
with error analyses for all reflection
data inversion techniques.

# VI. References

[1] May, B. T. and D. K. Straley,
Higher-order Moveout Spectra,
Geophysics, v. 44, n. 7, July, 1979.

[2] Taner, M. T. and F. Koehler, Veloc-
ity Spectra-Digital Computer Derivation
and Applications of Velocity Functions,
Geophysics, v. 34, n. 6, December, 1969.

[3] Rutherford, S. R., Analytical
Techniques for Determining Subbottom
Velocity Profiles in Unconsolidated
Sediments, Applied Research Labora-
tories, University of Texas Report No.
ARL-TR-76-58, 1976.

[4] Dix, C. H., Seismic Velocities from
Surface Measurements, Geophysics, v. 20,
n. 1, 1955.

[5] Gibson, B., M. Odegard and G.
Sutton, Nonlinear Least-Squares Inver-
sion of Traveltime Data for a Linear
Velocity Depth Relationship, Geo-
physics, v. 44, n. 2, February, 1979.

[6] Standard Mathematical Tables,
Chemical Rubber Co., 1964.

## Appendix A.
## Moments for Example Sound Speed Profiles

For the case where receiver depth is same as source depth $(D_1=0)$ equation (A.2a) reduces to

$$M_i = 2 \sum_{j=1}^{N} V_j^i H_j \qquad (A.2b)$$

### I. Series of Constant Sound Speed Layers

A sound speed versus depth relationship, $V_Z(z)$, consisting of N constant sound speed layers is shown in Figure A-1. From defining equation (1a) of the text, moments $M_i$ of the sound speed profile (for the given measurement configuration) are given by

$$M_i = \int_0^{D_N} V_Z^i(z) \, dz + \int_{D_1}^{D_N} V_Z^i(z) \, dz \qquad (A.1)$$

where $D_1$ is receiver depth and $D_N$ is depth of the reflecting boundary of interest. Substituting the sound speed profile, $V_Z(z)$, illustrated by Figure A-1 into equation (A.1), results in the following.

$$M_i = \sum_{j=1}^{N} \int_{D_{j-1}}^{D_j} V_j^i \, dz + \sum_{j=2}^{N} \int_{D_{j-1}}^{D_j} V_j^i \, dz$$

Sound speed, $V_j$, being constant over the specified integration intervals allows $M_i$ to be expressed by

$$M_i = \sum_{j=1}^{N} V_j^i(D_j - D_{j-1}) + \sum_{j=2}^{N} V_j^i(D_j - D_{j-1})$$

Rearranging, and noticing $(D_j - D_{j-1})$ is identically $H_j$, results in the more convenient form

$$M_1 = 2 \sum_{j=1}^{N} V_j^i H_j - V_1^i H_1 \qquad (A.2a)$$

Substituting the moments of equation (A.2b) into equations (20) of the text results in moveout, $T(x)$, polynomial coefficients which agree (to within obvious typographical errors) with that reported by Taner and Koehler [A1].

### II. Series of Constant Gradient Layers

A sound speed profile, $(V_Z(z))$, consisting of N constant *gradient* layers is shown in Figure A-2. From defining equation (1a) of the text, moments, $M_i$, of the sound speed profile (for the given measurement configuration) are given by

$$M_i = \int_0^{D_N} V_Z^i(z) \, dz + \int_{D_1}^{D_N} V_Z^i(z) \, dz \qquad (A.3)$$

where $D_1$ is receiver depth and $D_N$ is depth of the reflecting boundary of interest. Adopting the notation $Vt_j$ and $Vb_j$ are velocities at the "top" and "bottom", respectively, of layer j, allows the moments to be expressed by

$$M_i = 2 \sum_{j=1}^{N} \frac{1}{g_j} \ell n \left[ \frac{Vb_j}{Vt_j} \right] - \frac{1}{g_1} \ell n \left[ \frac{Vb_1}{Vt_1} \right] \text{ for } i=-1$$

$$(A.4a)$$

and

$$M_i = \frac{2}{(i+1)} \sum_{j=1}^{N} \frac{Vb_j^{i+1} - Vt_j^{i+1}}{g_j}$$

$$- \frac{(Vb_1^{i+1} - Vt_1^{i+1})}{g_1(i+1)} \text{ for } i \neq -1 . \qquad (A.4b)$$
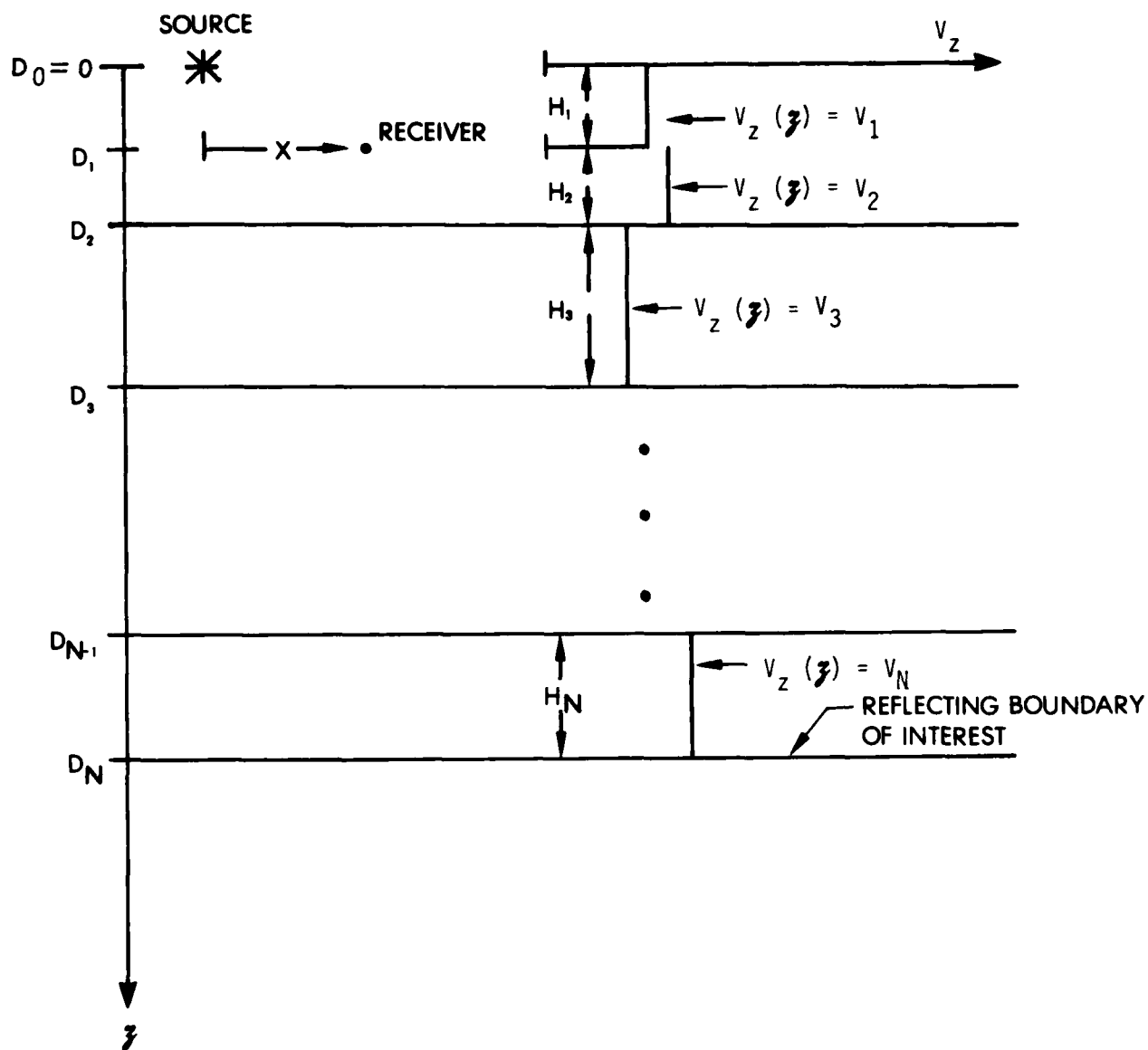
27

Figure A-1. Series of Constant Sound Speed Layers

Figure A-2. Series of Constant Gradient Layers

For the case where receiver depth is the
same as source depth ($D_1=0$) equations
(A.4) reduce to

$$M_i = 2 \sum_{j=1}^{N} \frac{1}{g_j} \ell n \left[ \frac{Vb_j}{Vt_j} \right] \text{ for } i=-1 \quad \text{and} \quad (A.5a)$$

$$M_i = \frac{2}{(i+1)} \sum_{j=1}^{N} \frac{Vb_j^{i+1} - Vt_j^{i+1}}{g_j} \text{ for } i \neq -1 . (A.5b)$$

## III. More General $V_z(z)$

Con inuing the list of examples is
som iat pointless, since it is
do tful that an example will fully
meet the requirements of an actual
application. Moments for more general
sound speed versus depth relationship
can be computed directly from defining
equations (1) of the text.

REFERENCES

[1] Taner, M.T. and Koehler, F., Veloc-
ity Spectra—Digital Computer Derivation
and Applications of Velocity Functions,
Geophysics, v. 34, n. 6, 1969.

# Appendix B.
## Derivation of $T^2(x)$ Polynomial

---

## I. Relating Coefficients to Derivatives

The "moveout" polynomial squared is approximated[†] by a finite order Taylor series about the normal incidence reflection travel path; viz.

$$T^{\cdot}(x) = C_0 + C_2 x^2 + C_4 x^4 + C_6 x^6 + C_8 x^8 \ldots \tag{B.1}$$

Coefficients of the expansion can be related to $T^2(x)$ and its derivatives to yield the following equations.

$$C = \lim_{x \to \cdot} T^{\cdot}(x) \tag{B.2a}$$

$$C = \lim_{x \to \cdot} \frac{dT^{\cdot}}{dx} \tag{B.2b}$$

$$C_{\cdot} = \lim_{x \to \cdot} \frac{1}{2} \frac{d}{dx} \left[ \frac{dT^{\cdot}}{dx^{\cdot}} \right] \tag{B.2c}$$

$$C = \lim_{x \to \cdot} \frac{1}{6} \frac{d}{dx} \left[ \frac{d}{dx^{\cdot}} \frac{dT^{\cdot}}{dx^{\cdot}} \right] \tag{B.2d}$$

$$C_N = \lim_{x \to \cdot} \frac{1}{N!} \frac{d^N}{d(x^{\cdot})^N} \left[ T^{\cdot} \right] \tag{B.2e}$$

## II. Notation

Deriving the derivative expression of equations (B.2) in terms of physical considerations (measurement geometry and sound speed versus depth, $V_Z(z)$) is greatly simplified by defining the following notation:

$$E_{i,j} \triangleq \int_0^{D.} \frac{V_Z^i(z)\, dz}{\cos^{j\cdot}(z)} + \int_{D_r}^{D_\ell} \frac{V_Z^i(z)\, dz}{\cos^{j}\theta(z)} \tag{B.3}$$

where

$z \triangleq$ Depth below source [see Fig. B-1]

$V_Z(z) =$ Sound speed at depth $z$ [see Fig. B-1]

$\theta_0 \triangleq$ Initial sound ray departure angle [see Fig. B-1]

$\theta(z) =$ Sound ray angle with respect to vertical at depth $z$ for an initial departure angle $\theta_0$ [see Fig. B-1]

$D_\ell \triangleq z$ coordinate of reflecting boundary of interest [see Fig. B-1]

$D_r \triangleq z$ coordinate of receiver [see Fig. B-1]

Differentiating equation (B.3) with respect to $\theta_0$ and applying Snell's law [$V_Z(0) \sin \theta(z) = V_Z(z) \sin \theta_0$] results in the following useful relationship.

$$E'_{i,j} \triangleq \frac{dE_{i,j}}{d\cdot} = Qj E_{i+\cdot,j+\cdot} \tag{B.4}$$

where

$$Q \cdot \frac{\sin \cdot \cos \cdot}{V_Z(0)}$$

Reflection path travel time and x direction travel distance as a function of sound ray initial departure angle $\theta_0$ can be expressed by [see Fig. B-1]
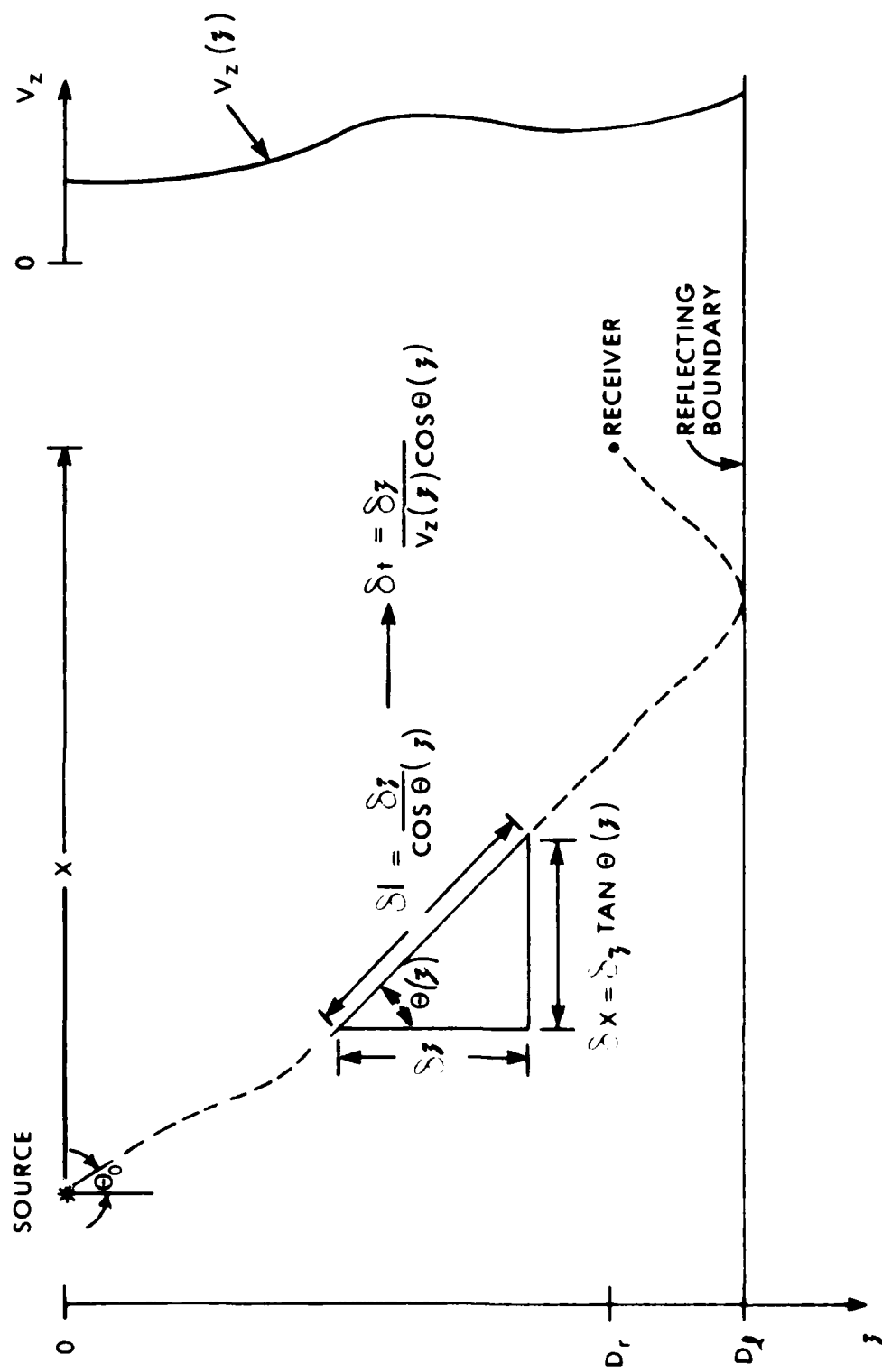
Figure B-1. General Configuration

$$x(\theta_0) = \int_0^{D_\ell} \frac{\sin\theta(z)}{\cos\theta(z)}\, dz + \int_{D_r}^{D_\ell} \frac{\sin\theta(z)}{\cos\theta(z)}\, dz \quad (B.5)$$

$$T(\theta_0) = \int_0^{D_\ell} \frac{dz}{V_Z(z)\cos\theta(z)} + \int_{D_r}^{D_\ell} \frac{dz}{V_Z(z)\cos\theta(z)} \quad (B.6)$$

Applying Snell's law $[V_Z(0)\sin\theta(z) = V_Z(z)\sin\theta_0]$ to equation (B.5) yields

$$x(\ ) = \frac{\sin}{V_Z(0)}\left[\int_0^{D} \frac{V_Z(z)dz}{\cos(z)}\, dz + \int_{D_r}^{D_\ell} \frac{V_Z(z)}{\cos\theta(z)}\, dz\right] . \quad (B.7)$$

Using the notation of defining equation (B.3), equations (B.6) and (B.7) and their derivatives with respect to $\theta_0$ can be expressed by

$$\ (\ ) \quad E_{\ } , \quad (B.8)$$

$$\frac{dT}{d} \quad QE \ , \quad \text{where } Q \quad \frac{\sin\ \cos}{V_Z(0)} \quad (B.9)$$

$$x\ \quad \frac{\sin}{V_Z(0)} E \ . \quad (B.10)$$

$$\frac{dx}{d} \quad \frac{\cos}{V_Z(0)} E \ , \quad (B.11)$$

The derivative $dT(x)/dx$ can now be evaluated quite easily. Expanding $dT/dx$ in terms of $dT/d\theta_0$ and $dx/d\theta_0$, and using equations (B.9) and (B.11) yields

$$\frac{dT}{dx} \quad \frac{dT/d}{dx/d} \quad \frac{\sin}{V_Z(0)} . \quad (B.12)$$

### III. Determining $C_0$

Coefficient $C_0$ is simply the normal incident reflection path (source to receiver x=0) travel time squared. Therefore, $C_0$ can be expressed as follows.

$$C_0 = T^2(0) = \left[\int_0^{D_\ell} \frac{dz}{V_Z(z)} + \int_{D_r}^{D_\ell} \frac{dz}{V_Z(z)}\right]^2 \quad (B.13)$$

Equation (B.13) can also be expressed in terms of moments by

$$C_0 = (M_{-1})$$

where moments, $M_i$, are defined by

$$M_i = \int_0^{D_\ell} V_Z^i(z)dz + \int_{D_r}^{D_\ell} V_Z^i(z)dz \quad (B.14)$$

### IV. Determining $C_2$

Coefficient $C_2$ is expressed in terms of $dT^2/dx^2$ in equation (B.2b). The derivative, $dT^2/dx^2$, can be expanded (by identity) to yield

$$\frac{dT}{dx} \quad \frac{T\, dT/dx}{x} . \quad (B.15)$$

Substituting equations (B.8), (B.10) and (B.12) into equation (B.15) yields the following expression for $dT^2/dx^2$.

$$\frac{dT}{dx} \quad \frac{E_{\ }}{E_{\ }} \quad (B.16)$$

Substituting equation (B.16) into (B.2b) yields

$$C \quad \lim_{x\ } \frac{E_{\ }}{E_{\ }} \quad (B.17)$$

The limit as $x \to 0$ in equation (B.17) is identically the same as the limit as $\theta_0 \to 0$. Incorporating this identity and the moments definition [see equation (B.14)] results in

$$C = \frac{M_{-1}}{M_{\cdot}} \quad . \tag{B.18}$$

## V. Determining $C_4$

From equation (B.2c), coefficient $C_4$ is given by

$$C_{\cdot} = \lim_{x \to 0} \frac{1}{2} \frac{d}{dx^{\cdot}} \left( \frac{dT^{\cdot}}{dx^{\cdot}} \right) . \tag{B.19}$$

To evaluate $d(dT^2/dx^2)/dx^2$, let $R_2$ be defined as $dT^2/dx^2$. This allows $d(dT^2/dx^2)/dx^2$ to be expressed by

$$\frac{d}{dx^{\cdot}} \left( \frac{dT^{\cdot}}{dx^{\cdot}} \right) = \frac{dR_{2}}{dx^{\cdot}} \quad \frac{1}{2} \frac{dR_2/dx}{x} \quad . \tag{B.20a}$$

Expanding $dR_2/dx$ in terms of $dR_2/d\theta_0$ and $dx/d\theta_0$ allows

$$\frac{d}{dx^{\cdot}} \left( \frac{dT^{\cdot}}{dx^{\cdot}} \right) = \frac{1}{2} \frac{dR_{\cdot}/d\theta_0}{x \, dx/d\theta_0} \quad . \tag{B.20b}$$

The variable $R_2$ is defined as $dT^2/dx^2$ which is related to "$E_{i,j}$" notation in equation (B.16). Incorporating the "$E_{i,j}$" notation allows

$$\frac{d}{dx^{\cdot}} \left( \frac{dT^{\cdot}}{dx^{\cdot}} \right) = \frac{1}{2} \frac{\dfrac{d}{d\theta_{\cdot}} \left( \dfrac{E_{-1,1}}{E_{1,1}} \right)}{x \, dx/d\theta_0} \tag{B.20c}$$

Expanding $\dfrac{d}{d\theta_{\cdot}} \left( \dfrac{E_{-1,1}}{E_{1,1}} \right)$ results in the following equation

$$\frac{d}{dx^{\cdot}} \left( \frac{dT^{\cdot}}{dx^{\cdot}} \right) = \frac{1}{2} \left[ \frac{\dfrac{E_{-1,1}^{\cdot}}{E_{1,1}} - \dfrac{E_{-1,1} \, E_{1,1}^{\cdot}}{E_{1,1}}}{x \, dx/d\theta_{\cdot}} \right]$$

where superscript $'$ denotes $\dfrac{d}{d\theta_0}$. Substituting for $E_{-1,1}^{\cdot}$ and $E_{1,1}^{\cdot}$ (see equation (B.4)) results in

$$\frac{d}{dx^{2}} \left( \frac{dT^{2}}{dx^{2}} \right) = \frac{\sin\theta_{0} \, \cos\theta_{0}}{2V_{z}^{2}(0)} \left[ \frac{\dfrac{E_{1,3}}{E_{1,1}} - \dfrac{E_{-1,1} \, E_{3,3}}{E_{1,1}^{2}}}{x \, dx/d\theta_{0}} \right] .$$

Substituting for $x$ and $dx/d\theta_0$ from equations (B.10) and (B.11) and rearranging results in the following expression for $d(dT^2/dx^2)/dx^2$

$$\frac{d}{dx^{2}} \left( \frac{dT^{2}}{dx^{2}} \right) = \frac{1}{2} \left[ \frac{1}{E_{1,1}^{2}} - \frac{E_{-1,1} \, E_{3,3}}{E_{1,1}^{3} \, E_{1,1}} \right] \tag{B.21}$$

Taking the limit as $x$ goes to zero and substituting into equation (B.2c) results in the following expression for $C_4$ in terms of moments.

$$C_{\cdot} = \frac{1}{4M_{1}^{2}} \left[ 1 - \frac{M_{-1} \, M_{3}}{M_{1}^{2}} \right] \tag{B.22}$$

## VI. Determining $C_6$

From equation (B.2d), coefficient $C_6$ is given by

$$C_{6} = \lim_{x \to 0} \frac{1}{6} \frac{d}{dx^{2}} \left( \frac{d}{dx^{\cdot}} \frac{dT^{\cdot}}{dx^{\cdot}} \right) \tag{B.23}$$

Defining $R_4$ as $d(dT^2/dx^2)/dx^2$, which is given by equation (B.21), allows the derivatives of equation (B.23) to be expressed as

$$\frac{d}{dx^{\cdot}} \left( \frac{d}{dx^{\cdot}} \frac{dT^{\cdot}}{dx^{\cdot}} \right) = \frac{d}{dx^{\cdot}} R_{\cdot} \quad . \tag{B.24a}$$

Following the same steps as in the previous section from equations (B.20a) to (B.20c), results in the following

$$\frac{d}{dx^{2}} \left( \frac{d}{dx^{\cdot}} \frac{dT^{2}}{dx^{\cdot}} \right) = \left[ \frac{1}{2x \dfrac{dx}{d\theta_{0}}} \right]$$

$$\cdot \left[ \frac{d}{d\theta_{0}} \frac{1}{2} \left( \frac{1}{E_{1,1}^{\cdot}} - \frac{E_{-1,1} \, E_{3,3}}{E_{1,1} \, E_{1,1}} \right) \right] \tag{B.24b}$$

34

Rearranging and substituting for x and $dx/d\theta_0$ from equations (B.10) and (B.11) results in

$$\frac{d}{dx^2}\left(\frac{d}{dx^2}\frac{dT^2}{dx^2}\right) = \left[\frac{V_Z^2(0)}{4\sin\theta_0\cos\theta_0\ E_{1,1}\ E_{1,3}}\right]$$

$$\cdot\left[\frac{d}{d\theta_0}\left(E_{1,1}^{-2} - E_{-1,1}\ E_{3,3}\ E_{1,1}^{-1}\ E_{1,3}^{-1}\right)\right] \quad (B.24c)$$

Performing the indicated differentiation with respect to $\theta_0$ yields the following equation for $d[d(dT^2/dx^2)/dx^2]/dx^2$

$$\frac{d}{dx^2}\left(\frac{d}{dx^2}\frac{dT^2}{dx^2}\right) = \left[\frac{3}{4\ E_{1,1}^4\ E_{1,3}^2}\right]\cdot\left[-E_{1,3}\ E_{3,3}\right.$$

$$\left. - E_{5,5}\ E_{-1,1} + \frac{E_{3,3}^2\ E_{-1,1}}{E_{1,1}} + \frac{E_{3,5}\ E_{-1,1}\ E_{3,3}}{E_{1,3}}\right]$$

$$(B.25)$$

Taking the limit as x approachs zero, and substituting into equation (B.23) yields the following equation for $C_6$

$$C_6 = \frac{1}{8M_1^6}\left[\frac{2M_3\ M_{-1}}{M_1} - M_3\ M_3 - M_5\ M_{-1}\right] \quad (B.26)$$

## VII. Determining $C_8$

Coefficient $C_8$ can be derived using a procedure identical to that for lower order coefficients. For brevity, only the result is shown here

$$C_8 = \frac{1}{64M_1^9}\left[9M_3^2 M_1 + 24M_3\ M_5\ M_{-1}\right.$$

$$\left. - \frac{24M_3^3\ M_{-1}}{M_1} - 4M_5\ M_1^2 - 5M_7\ M_{-1}\ M_1\right] \quad (B.27)$$

## VIII. Summary

The polynomial moveout coefficients are related to moments by the following expressions

$$C_0 = (M_{-1})^2$$

$$C_2 = \frac{M_{-1}}{M_1}$$

$$C_4 = \frac{1}{4M_1^2}\left[1 - \frac{M_{-1}\ M_3}{M_1^2}\right]$$

$$C_6 = \frac{1}{8M_1^6}\left[\frac{2M_3^2\ M_{-1}}{M_1} - M_1\ M_3 - M_5\ M_{-1}\right]$$

$$C_8 = \frac{1}{64M_1^9}\left[9M_3^2\ M_1 + 24M_3\ M_5\ M_{-1}\right.$$

$$\left. - \frac{24M_3^3\ M_{-1}}{M_1} - 4M_5\ M_1^2 - 5M_7\ M_{-1}\ M_1\right]$$

where the moments, $M_i$, are defined by

$$M_i \triangleq \int_0^{D_\ell} V_Z^i(\mathbf{z})d\mathbf{z} + \int_{D_r}^{D_\ell} V_Z^i(\mathbf{z})d\mathbf{z} .$$

# Distribution List

002 0000 000 A1 ASN(RE&S)
Department of the Navy
Asst Secretary of the Navy
(Research Engineering & Systems)
Washington DC    20350


298 0000 000 A2A ONR
Department of the Navy
Office of Naval Research
ATTN:   Code 102
800 N Quincy St
Arlington VA    22217


245 0000 000 HCAFA/ONRDET
Director
Chief of Naval Research
ONR Code 480
Ocean Science & Technology Det
NSTL Station, MS    39529


004 0000 000 A3 CNO
Department of the Navy
Chief of Naval Operations
ATTN:   OP0951
Washington DC    20350


004 0000 000 A3 CNO
Department of the Navy
Chief of Naval Operations
ATTN:   OP 952
Washington DC    20350


004 0000 000 A3 CNO
Department of the Navy
Chief of Naval Operations
ATTN:   OP 980
Washington DC    20350


005 0000 000 A4A CHNAVMAT
Department of the Navy
Chief of Naval Material
Washington DC    20360


095 0000 000 C4K PM-4
Project Manager
ASW Systems Project (PM-4)
Department of the Navy
Washington DC    20362


098 5520 750 C4L DNL
Department of the Navy
Director Of Navy Laboratories
Rm 1062 Crystal Plaza Bldg 5
Washington DC    20360


047 3860 930 E3A NRL
Commanding Officer
Naval Research Laboratory
Washington DC    20375


068 5580 350 E3B ONRBRO
Commanding Officer
ONR Branch Office LONDON
Box 39
FPO New York    09510


067 5580 215 E3B ONRBRO
Commanding Officer
ONR Branch Office
536 S Clark Street
Chicago IL    50605


066 5581 210 E3B ONREAST
Commanding Officer
ONR Eastern/Central Reg Ofs
Bldg 114 Section D
666 Summer St
Boston MA    02210


069 5580 540 E3B ONRWEST
Commanding Officer
ONR Western Regional Ofs
1030 E. Green Street
Pasadena CA    91106


250 4480 200 E3C
Director, Liaison Office
Naval Ocean R&D Activity
800 N Quincy Street
502 Ballston Tower #1
Arlington VA    22217


053 4080 100 FD1 HCAFA/OCEANAV
Commander
Naval Oceanography Command
NSTL Station
Bay St. Louis MS    39522

062 4484 365 FD2 HCAFA/NAVOCEANO
Commanding Officer
Naval Oceanographic Office
NSTL Station
Bay St. Louis MS    39522

059 4483 270 FD3 FLENUMOCEANCEN
Commanding Officer
Fleet Numerical Ocean Cen
Monterey CA    93940

007 1461 900 FKA1A COMNAVAIRSYSCOM
Commander
Naval Air Systems Command
Headquarters
Washington DC    20361

023 2925 905 FKA1B COMNAVELEXSYSCOM
Commander
Naval Electronic Sys Com
Headquarters
Washington DC    20360

031 3075 910 FKA1C COMNAVFACENGCOM
Commander
Naval Facilities Eng Command
Headquarters
200 Stovall St.
Alexandria VA    22332

070 5765 900 FKA1G COMNAVSEASYSCOM
Commander
Naval Sea System Command
Headquarters
Washington DC    20362

006 1303 500 FKA6A1 NAVAIRDEVCEN
Commander
Naval Air Development Center
Warminster PA    18974

065 4489 800 FKA6A12 NAVOCEANSYSCOM.
Commander
Naval Ocean Systems Center
San Diego CA    92152

076 5541 500 FKA6A15 NUSC
Commanding Officer
Naval Underwater Systems Center
ATTN:  New London Lab (1 cy)
Newport RI    02840

071 5856 900 FKA6A3A DTNSRDC
Commander
DWTaylor Naval Ship R&D Cen
Bethesda MD    20034

009 2130 600 FKA6A3B NAVCOASTSYSCEN
Commanding Officer
Naval Coastal Systems Center
Panama City FL    32407

074 6214 950 FKA6A9 NAVSWC
Commander
Naval Surface Weapons Center
Dahlgren VA    22448

030 2980 500 FKR8C NAVENVPREDRSCHFAC
Commanding Officer
Naval Environmental Prediction
Research Facility
Monterey CA    93940

085 7685 435 FT73 NAVPGSCOL
Superintendent
Naval Postgraduate School
Monterey CA    93940

800 0000 000
President
Woods Hole Oceanographic Inst
Woods Hole MA    20543

304 0000 000
Director
Scripps Inst of Oceanography
Univ of Southern California
La Jolla CA    92093

136 0000 000 000 DTIC
Director
Defense Technology Info Cen
Cameron Station
Alexandria VA    22314

045 3860 200 E3C NORDA
Commanding Officer
Naval Ocean R & D Activity
ATTN: Codes 100/110
NSTL Station MS 39529

045 3860 200 E3C NORDA
Commanding Officer
Naval Ocean R & D Activity
ATTN: Code 125L
NSTL Station MS 39529

045 3860 200 E3C NORDA
Commanding Officer
Naval Ocean R & D Activity
ATTN: Code 125 Tech Ed
NSTL Station MS 39529

045 3860 200 E3C NORDA
Commanding Officer
Naval Ocean R & D Activity
ATTN: Code 300
NSTL Station MS 39529

045 3860 200 E3C NORDA
Commanding Officer
Naval Ocean R & D Activity
ATTN: Code 115
NSTL Station MS 39529

045 3860 200 E3C NORDA
Commanding Officer
Naval Ocean R & D Activity
ATTN: Code 500
NSTL Station MS 39529

074 6214 950 FKA6A9 NAVSWC
Commander
Naval Surface Weapons Center
Attn: Dr. E. L. Price
Dahlgren VA 22448

McAdams, Roux, O'Connor Associates,
Inc.
300 Equitable Bldg
730 Seventeenth Street
ATTN: Dr. Bruce T. May
Devner CO 80202

Dr. Alfred Behle
Professor of Geophysics
Inisitute of Geophysics
University of Hamburg
Bundesstr, 55
D-2000 Hamburg 13
WEST GERMANY

38

| REPORT DOCUMENTATION PAGE | | READ INSTRUCTIONS<br>BEFORE COMPLETING FORM |
|---|---|---|
| 1. REPORT NUMBER<br>NORDA Report 30 | 2. GOVT ACCESSION NO.<br>AD-A099 816 | 3. RECIPIENT'S CATALOG NUMBER |
| 4. TITLE (and Subtitle)<br>A Moments Approach for Analyzing Geophysical<br>Reflection Data | | 5. TYPE OF REPORT & PERIOD COVERED |
| | | 6. PERFORMING ORG. REPORT NUMBER |
| 7. AUTHOR(s)<br>Norman H. Gholson<br>Martin G. Fagot | | 8. CONTRACT OR GRANT NUMBER(s) |
| 9. PERFORMING ORGANIZATION NAME AND ADDRESS<br>Naval Ocean Research & Development Activity<br>Ocean Science & Technology Laboratory, Code 350<br>NSTL Station, Mississippi 39529 | | 10. PROGRAM ELEMENT, PROJECT, TASK<br>AREA & WORK UNIT NUMBERS |
| 11. CONTROLLING OFFICE NAME AND ADDRESS<br>Naval Ocean Research & Development Activity<br>Ocean Technology Division, Code 350<br>NSTL Station, Mississippi 39529 | | 12. REPORT DATE<br>May 1980 |
| | | 13. NUMBER OF PAGES<br>41 |
| 14. MONITORING AGENCY NAME & ADDRESS(if different from Controlling Office) | | 15. SECURITY CLASS. (of this report)<br>UNCLASSIFIED |
| | | 15a. DECLASSIFICATION/DOWNGRADING<br>SCHEDULE |

16. DISTRIBUTION STATEMENT (of this Report)

Distribution Unlimited

17. DISTRIBUTION STATEMENT (of the abstract entered in Block 20, if different from Report)

18. SUPPLEMENTARY NOTES

19. KEY WORDS (Continue on reverse side if necessary and identify by block number)

20. ABSTRACT (Continue on reverse side if necessary and identify by block number)
This publication presents a new approach developed for analyzing geophysical
acoustic reflecting data. The forward problem of estimating source to receiver
travel time, and the inverse problem of estimating a sound speed versus depth
relationship are addressed using a moments approach. The moments approach pro-
vides a simple tool for estimating source to receiver reflection path travel
time for a laterally homogeneous medium with an arbitrary sound speed versus
depth relationship. The moments approach also provides a useful tool for in-

inverting reflection data to obtain an estimate of the sound speed versus depth
relationship. A nearly closed form technique for estimating a linear sound
speed versus depth relationship is presented. Derivation of the moments
approach and numerical examples are included.

DATE

ILME